

The Nikhef logo consists of the word "Nikhef" in a white, sans-serif font, with a stylized white symbol above the letter "i" that resembles a particle detector or a branching structure.The logo for the University of Amsterdam, featuring a white square icon with a stylized 'U' and 'A' and the text "UNIVERSITY OF AMSTERDAM" in a white, sans-serif font.

Big Bang Nucleosynthesis constraints on **resonant** DM annihilations

Pieter Braat

Work together with Marco Hufnagel

60th International School on Subnuclear Physics

Erice

Photodisintegration

Short recap: Big Bang Nucleosynthesis is the process in which abundances of the **lightest elements** are produced

and: observations match theory predictions

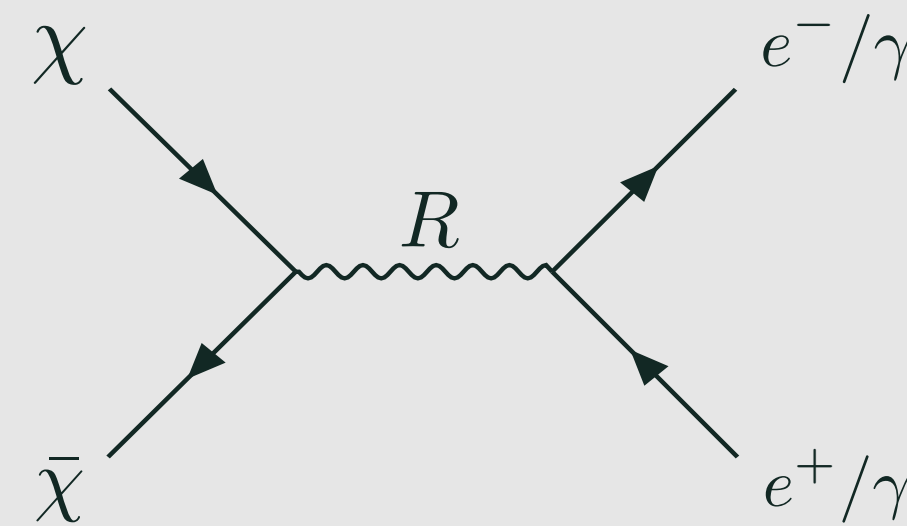
Photodisintegration

Short recap: Big Bang Nucleosynthesis is the process in which abundances of the **lightest elements** are produced

and: observations match theory predictions

EM **energy injection** (from BSM Physics) can **destroy** the newly formed elements

e.g. DM annihilations $\chi\bar{\chi} \rightarrow e^-e^+/\gamma\gamma$



Cascade equations

Solve the **cascade equations** for $X \in \{\gamma, e^-, e^+\}$

$$f_X(E) = \frac{1}{\Gamma_X(E)} \left(\underbrace{S_X(E)}_{\text{source term}} + \int_E^\infty dE' \sum_{X'} \underbrace{K_{X' \rightarrow X}(E, E') f_{X'}(E')}_{\text{conversion/scattering}} \right)$$

Cascade equations

Solve the **cascade equations** for $X \in \{\gamma, e^-, e^+\}$

$$f_X(E) = \frac{1}{\Gamma_X(E)} \left(\underbrace{S_X(E)}_{\text{source term}} + \int_E^\infty dE' \sum_{X'} \underbrace{K_{X' \rightarrow X}(E, E') f_{X'}(E')}_{\text{conversion/scattering}} \right)$$

Source term contains **monochromatic** and **final state radiation (FSR)** contribution

$$S_X(E) = S_X^{(0)} \delta(E - m_\chi) + S_X^{\text{FSR}}(E)$$

Monochromatic injection depends on the **coupling** to photons/electrons

$$S_X^{(0)} \propto n_\chi^2 \langle \sigma v \rangle_{\chi\chi \rightarrow XX}$$

Final state radiation source accounts for $\chi\chi \rightarrow e^+e^-\gamma$ interactions

$$S_\gamma^{\text{FSR}} \propto n_\chi^2 \langle \sigma v \rangle_{\chi\chi \rightarrow e^+e^-}$$

Cascade equations

Solve the **cascade equations** for $X \in \{\gamma, e^-, e^+\}$

$$f_X(E) = \frac{1}{\Gamma_X(E)} \left(\underbrace{S_X(E)}_{\text{source term}} + \int_E^\infty dE' \sum_{X'} \underbrace{K_{X' \rightarrow X}(E, E') f_{X'}(E')}_{\text{conversion/scattering}} \right)$$

Source term contains **monochromatic** and **final state radiation** (FSR) contribution

$$S_X(E) = S_X^{(0)} \delta(E - m_\chi) + S_X^{\text{FSR}}(E)$$

Monochromatic injection depends on the **coupling** to photons/electrons

$$S_X^{(0)} \propto n_\chi^2 \langle \sigma v \rangle_{\chi\chi \rightarrow XX}$$

Final state radiation source accounts for $\chi\chi \rightarrow e^+e^-\gamma$ interactions

$$S_\gamma^{\text{FSR}} \propto n_\chi^2 \langle \sigma v \rangle_{\chi\chi \rightarrow e^+e^-}$$

The injected particles **scatter** via interactions:

- $\gamma\gamma_{\text{th}} \rightarrow e^+e^-$
- $\gamma\gamma_{\text{th}} \rightarrow \gamma\gamma$
- $\gamma N \rightarrow Ne^+e^-$
- $\gamma e_{\text{th}}^- \rightarrow \gamma e^-$
- $e^\pm \gamma_{\text{th}} \rightarrow e^\pm \gamma$

Tracking the abundances

Light element abundances $N \in \{n, p, D, {}^3\text{H}, {}^3\text{He}, {}^4\text{He}, {}^7\text{Li}, {}^7\text{Be}\}$ are tracked via

$$\frac{dY_N}{dt} = \underbrace{\sum_{N_i} Y_{N_i} \int_0^\infty dE f_\gamma(E) \sigma_{\gamma+N_i \rightarrow N}(E)}_{\text{creation}} - \underbrace{Y_N \sum_{N_f} \int_0^\infty dE f_\gamma(E) \sigma_{\gamma+N \rightarrow N_f}(E)}_{\text{destruction}}$$

No.		E^{th} [MeV]
1	$D + \gamma \rightarrow p + n$	2.22
2	${}^3\text{H} + \gamma \rightarrow D + n$	6.26
3	${}^3\text{H} + \gamma \rightarrow p + n + n$	8.48
4	${}^3\text{He} + \gamma \rightarrow D + p$	5.49
5	${}^3\text{He} + \gamma \rightarrow n + p + p$	7.12
6	${}^4\text{He} + \gamma \rightarrow {}^3\text{H} + p$	19.81
7	${}^4\text{He} + \gamma \rightarrow {}^3\text{He} + n$	20.58
8	${}^4\text{He} + \gamma \rightarrow D + D$	23.84
9	${}^4\text{He} + \gamma \rightarrow D + n + p$	26.07

Tracking the abundances

- $\gamma\gamma_{\text{th}} \rightarrow e^+e^-$
- $\gamma\gamma_{\text{th}} \rightarrow \gamma\gamma$
- $\gamma N \rightarrow Ne^+e^-$
- $\gamma e_{\text{th}}^- \rightarrow \gamma e^-$
- $e^\pm \gamma_{\text{th}} \rightarrow e^\pm \gamma$

Light element abundances $N \in \{n, p, \text{D}, {}^3\text{H}, {}^3\text{He}, {}^4\text{He}, {}^7\text{Li}, {}^7\text{Be}\}$ are tracked via

Photodisintegration is sensitive to specific temperature range $T \in [10^{-7}, 10^{-2}]$ MeV : well after standard BBN has ended

$$\frac{dY_N}{dt} = \underbrace{\sum_{N_i} Y_{N_i} \int_0^\infty dE f_\gamma(E) \sigma_{\gamma+N_i \rightarrow N}(E)}_{\text{creation}} - \underbrace{Y_N \sum_{N_f} \int_0^\infty dE f_\gamma(E) \sigma_{\gamma+N \rightarrow N_f}(E)}_{\text{destruction}}$$

No.		E^{th} [MeV]
1	$\text{D} + \gamma \rightarrow p + n$	2.22
2	${}^3\text{H} + \gamma \rightarrow \text{D} + n$	6.26
3	${}^3\text{H} + \gamma \rightarrow p + n + n$	8.48
4	${}^3\text{He} + \gamma \rightarrow \text{D} + p$	5.49
5	${}^3\text{He} + \gamma \rightarrow n + p + p$	7.12
6	${}^4\text{He} + \gamma \rightarrow {}^3\text{H} + p$	19.81
7	${}^4\text{He} + \gamma \rightarrow {}^3\text{He} + n$	20.58
8	${}^4\text{He} + \gamma \rightarrow \text{D} + \text{D}$	23.84
9	${}^4\text{He} + \gamma \rightarrow \text{D} + n + p$	26.07

Tracking the abundances

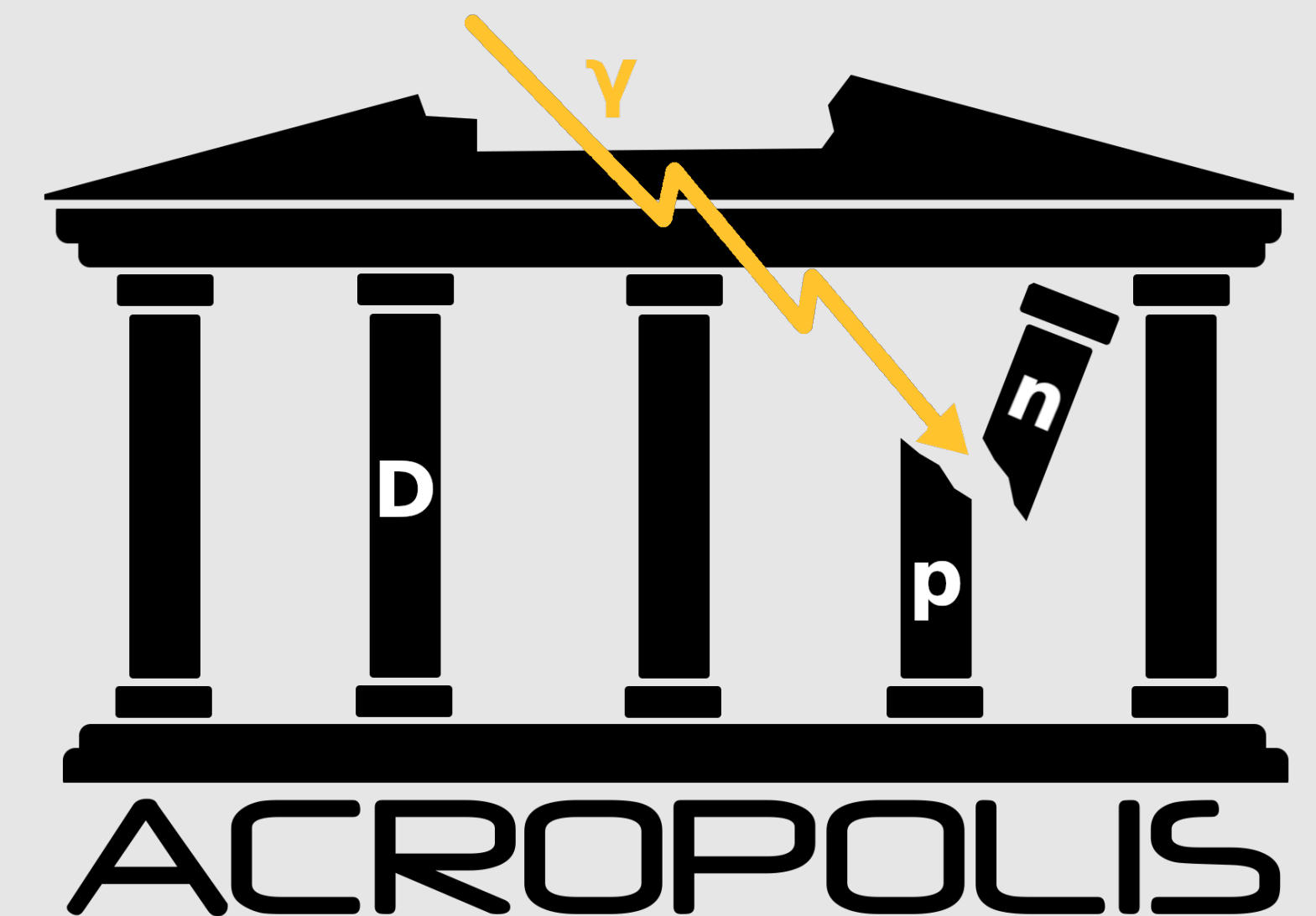
- $\gamma\gamma_{\text{th}} \rightarrow e^+e^-$
- $\gamma\gamma_{\text{th}} \rightarrow \gamma\gamma$
- $\gamma N \rightarrow Ne^+e^-$
- $\gamma e_{\text{th}}^- \rightarrow \gamma e^-$
- $e^\pm \gamma_{\text{th}} \rightarrow e^\pm \gamma$

Light element abundances $N \in \{n, p, \text{D}, {}^3\text{H}, {}^3\text{He}, {}^4\text{He}, {}^7\text{Li}, {}^7\text{Be}\}$ are tracked via

$$\frac{dY_N}{dt} = \underbrace{\sum_{N_i} Y_{N_i} \int_0^\infty dE f_\gamma(E) \sigma_{\gamma+N_i \rightarrow N}(E)}_{\text{creation}} - \underbrace{Y_N \sum_{N_f} \int_0^\infty dE f_\gamma(E) \sigma_{\gamma+N \rightarrow N_f}(E)}_{\text{destruction}}$$

No.		E^{th} [MeV]
1	$\text{D} + \gamma \rightarrow p + n$	2.22
2	${}^3\text{H} + \gamma \rightarrow \text{D} + n$	6.26
3	${}^3\text{H} + \gamma \rightarrow p + n + n$	8.48
4	${}^3\text{He} + \gamma \rightarrow \text{D} + p$	5.49
5	${}^3\text{He} + \gamma \rightarrow n + p + p$	7.12
6	${}^4\text{He} + \gamma \rightarrow {}^3\text{H} + p$	19.81
7	${}^4\text{He} + \gamma \rightarrow {}^3\text{He} + n$	20.58
8	${}^4\text{He} + \gamma \rightarrow \text{D} + \text{D}$	23.84
9	${}^4\text{He} + \gamma \rightarrow \text{D} + n + p$	26.07

Photodisintegration is sensitive to specific temperature range $T \in [10^{-7}, 10^{-2}]$ MeV : well after standard BBN has ended



In principle complicated system to solve → ACROPOLIS

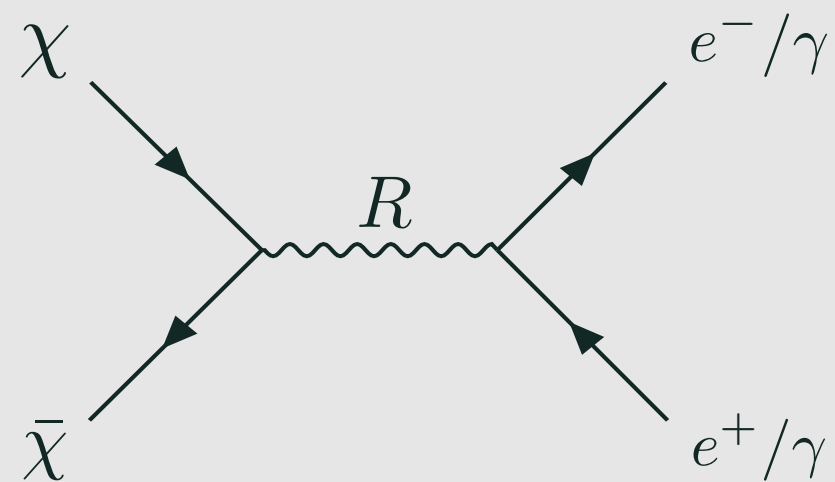
Depta, Hufnagel, Schmidt-Hoberg (2021)

Why resonant annihilations?

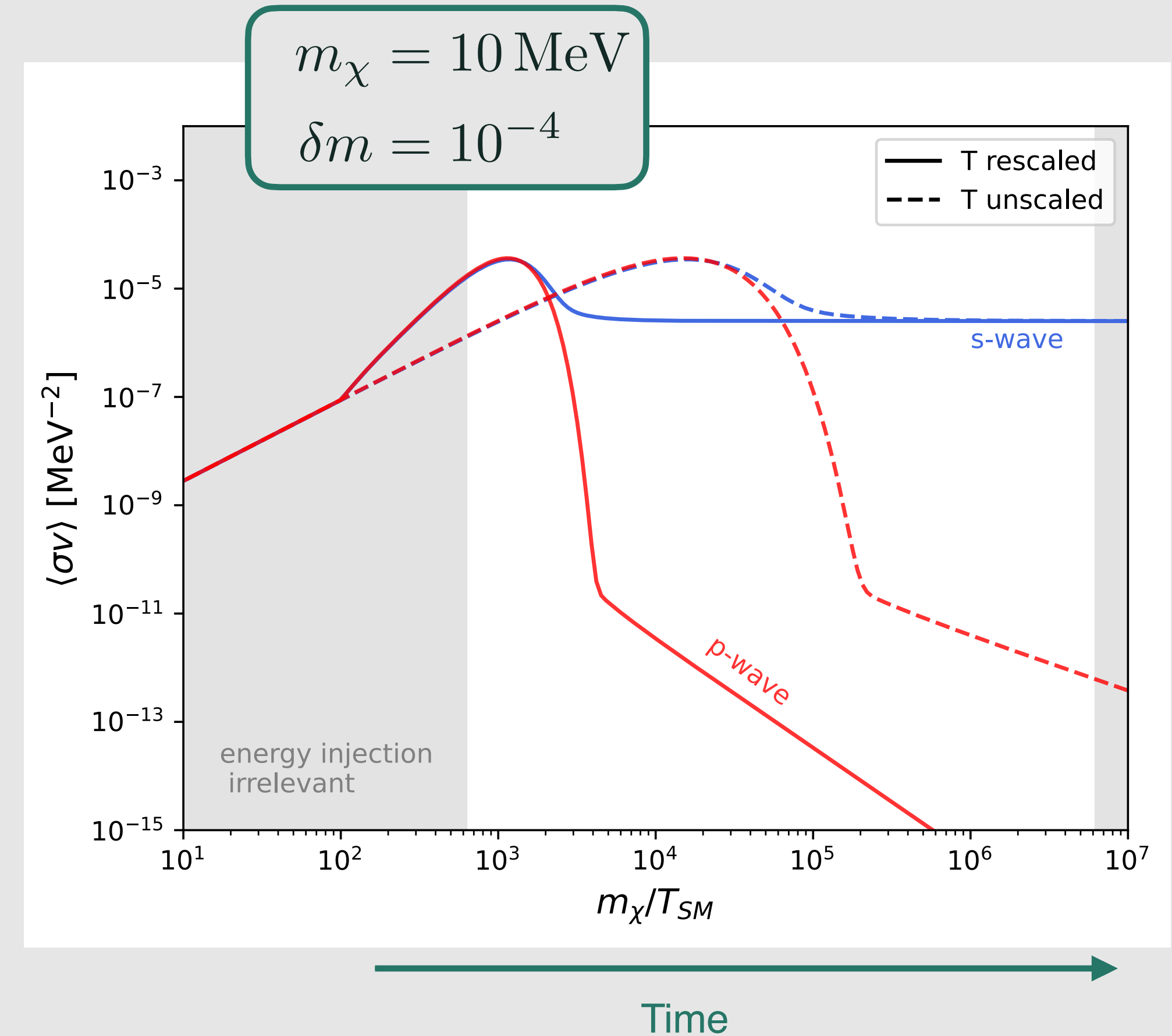
Consider dark sector with **resonance**

$$m_R \equiv m_\chi(2 + \delta m), \quad \delta m \ll 1$$

For **MeV scale DM**, annihilations **peak** in photodisintegration window!



Injected power



Why resonant annihilations?

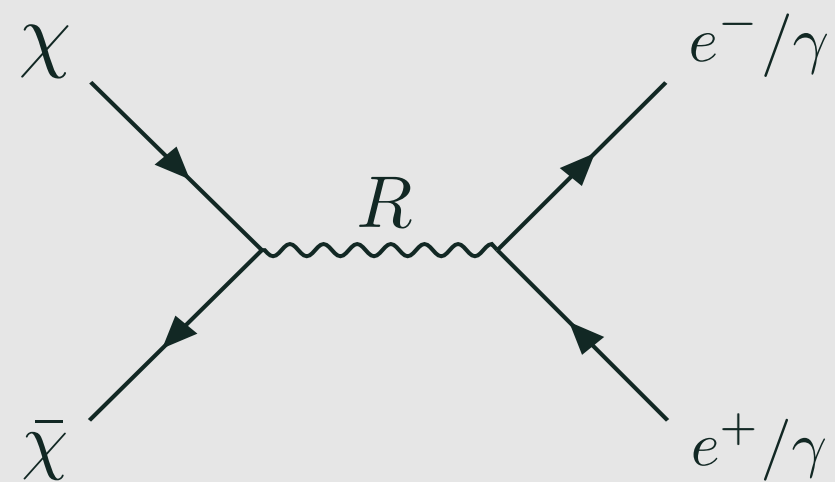
Consider dark sector with **resonance**

$$m_R \equiv m_\chi(2 + \delta m), \quad \delta m \ll 1$$

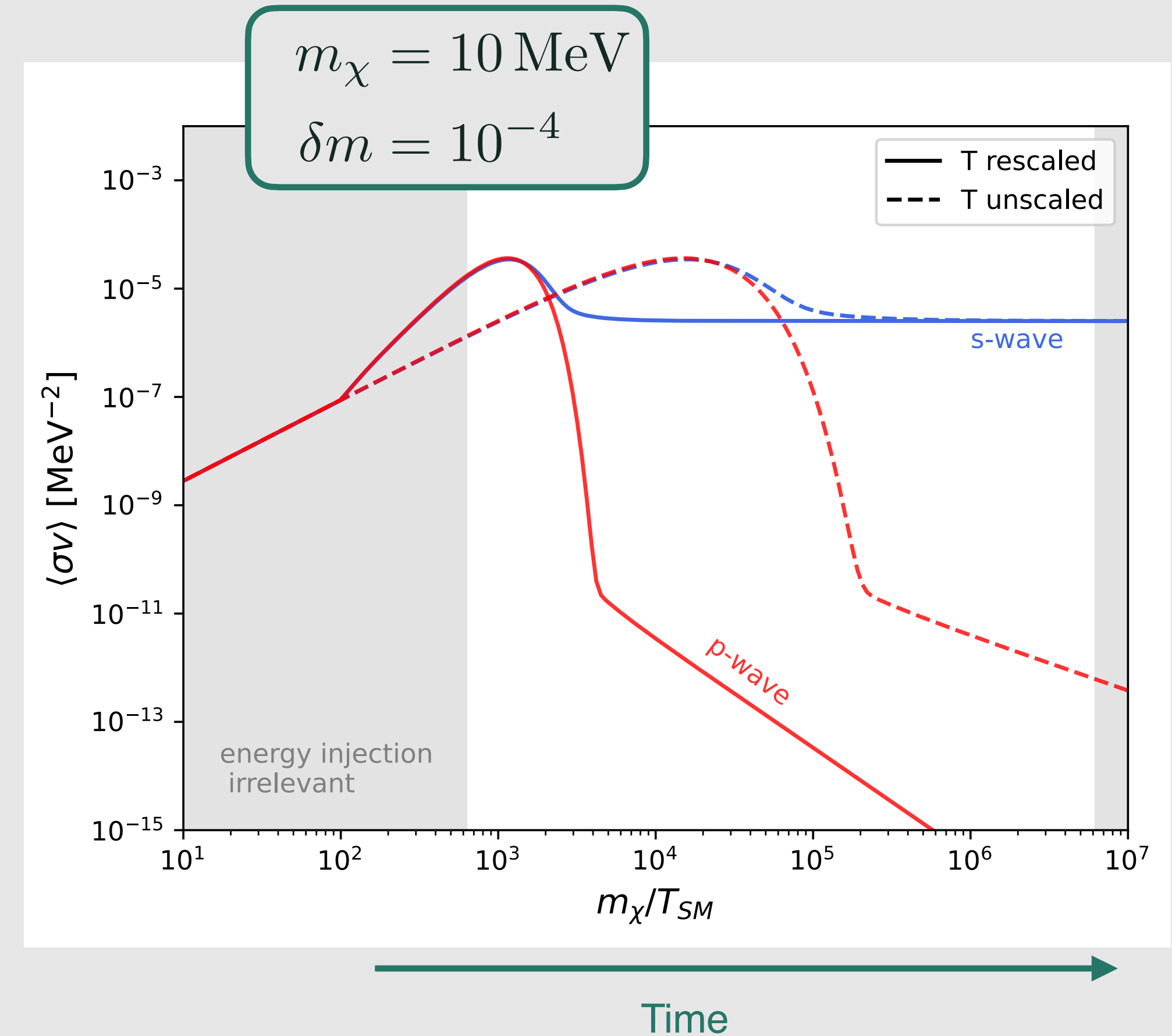
For **MeV scale DM**, annihilations **peak** in photodisintegration window!

We can write the **annihilation cross section** as

$$\sigma_{\text{ann}}^{\text{res}} = \frac{4\pi S}{m_\chi E(v)} \frac{\Gamma_d(v)\Gamma_v(v_f)/4}{(E(v) - E(v_R))^2 + \Gamma(v)^2/4}, \quad v_R \equiv 2\sqrt{\delta m}$$



Injected power



Why resonant annihilations?

Consider dark sector with **resonance**

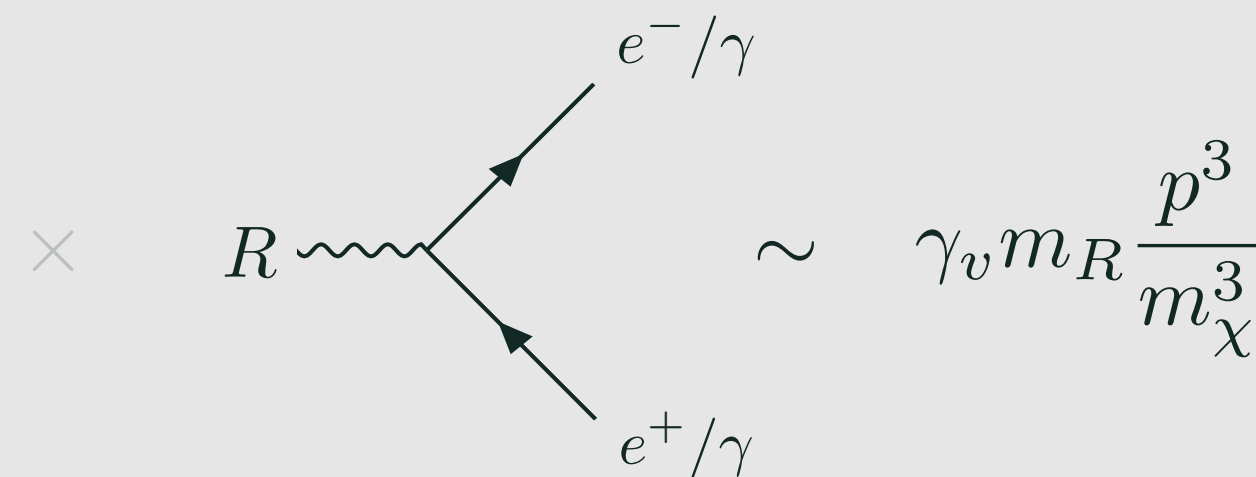
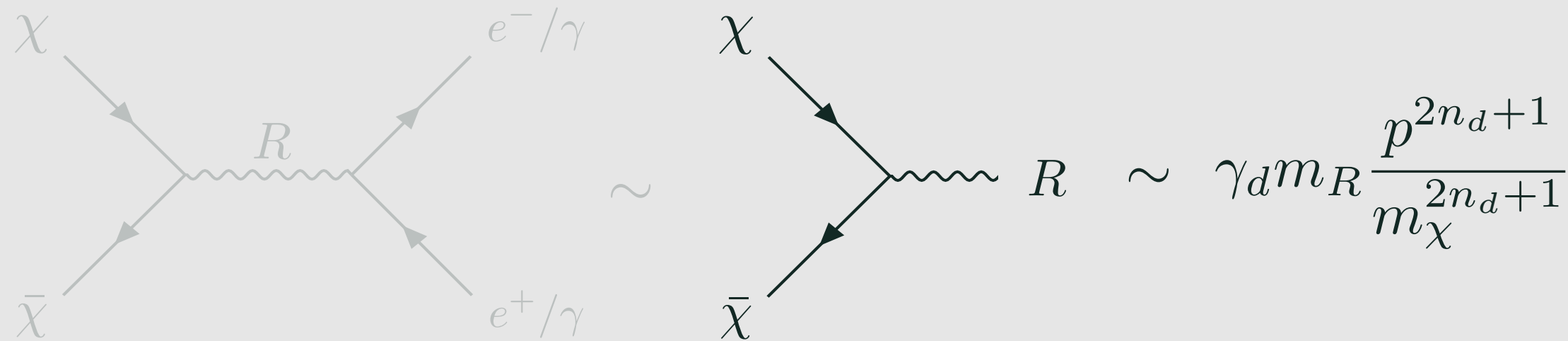
$$m_R \equiv m_\chi(2 + \delta m), \quad \delta m \ll 1$$

For **MeV scale DM**, annihilations **peak** in photodisintegration window!

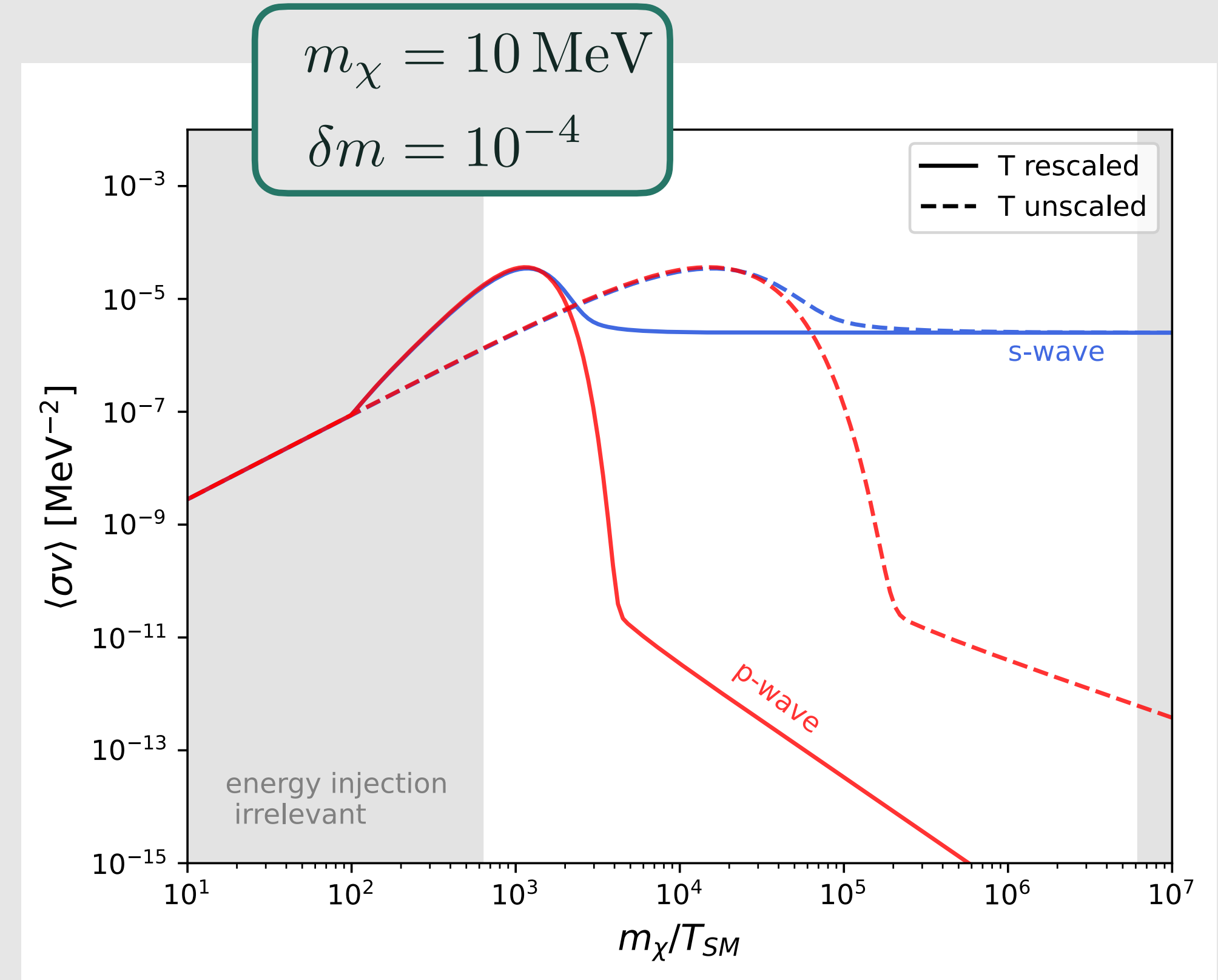
We can write the **annihilation cross section** as

$$\sigma_{\text{ann}}^{\text{res}} = \frac{4\pi S}{m_\chi E(v)} \frac{\Gamma_d(v)\Gamma_v(v_f)/4}{(E(v) - E(v_R))^2 + \Gamma(v)^2/4}, \quad v_R \equiv 2\sqrt{\delta m}$$

Injected power



- γ_d : dark coupling
- γ_v : visible coupling
- $n_d = 0$ s-wave
- $n_d = 1$ p-wave



Time

Model independent setup!

Temperature dependence

Injected energy depends on the **thermally averaged cross section**

$$\langle \sigma v \rangle_{\text{ann}} \stackrel{T_\chi \ll m_\chi}{=} \frac{4T_\chi^{3/2}}{\sqrt{\pi} m_\chi^{11/2}} \int_0^\infty dp^2 e^{-p^2 T_\chi / m_\chi^2} p^2 \sigma$$

with **DM temperature**

$$T_\chi(T) = \begin{cases} T & \text{if } T > T_{\text{kd}} \\ T_{\text{kd}} R(T_{\text{kd}})^2 / R(T)^2 & \text{if } T < T_{\text{kd}} \end{cases}$$

Temperature dependence

Injected energy depends on the **thermally averaged cross section**

$$\langle \sigma v \rangle_{\text{ann}} \stackrel{T_\chi \ll m_\chi}{=} \frac{4T_\chi^{3/2}}{\sqrt{\pi}m_\chi^{11/2}} \int_0^\infty dp^2 e^{-p^2 T_\chi / m_\chi^2} p^2 \sigma$$

with **DM temperature**

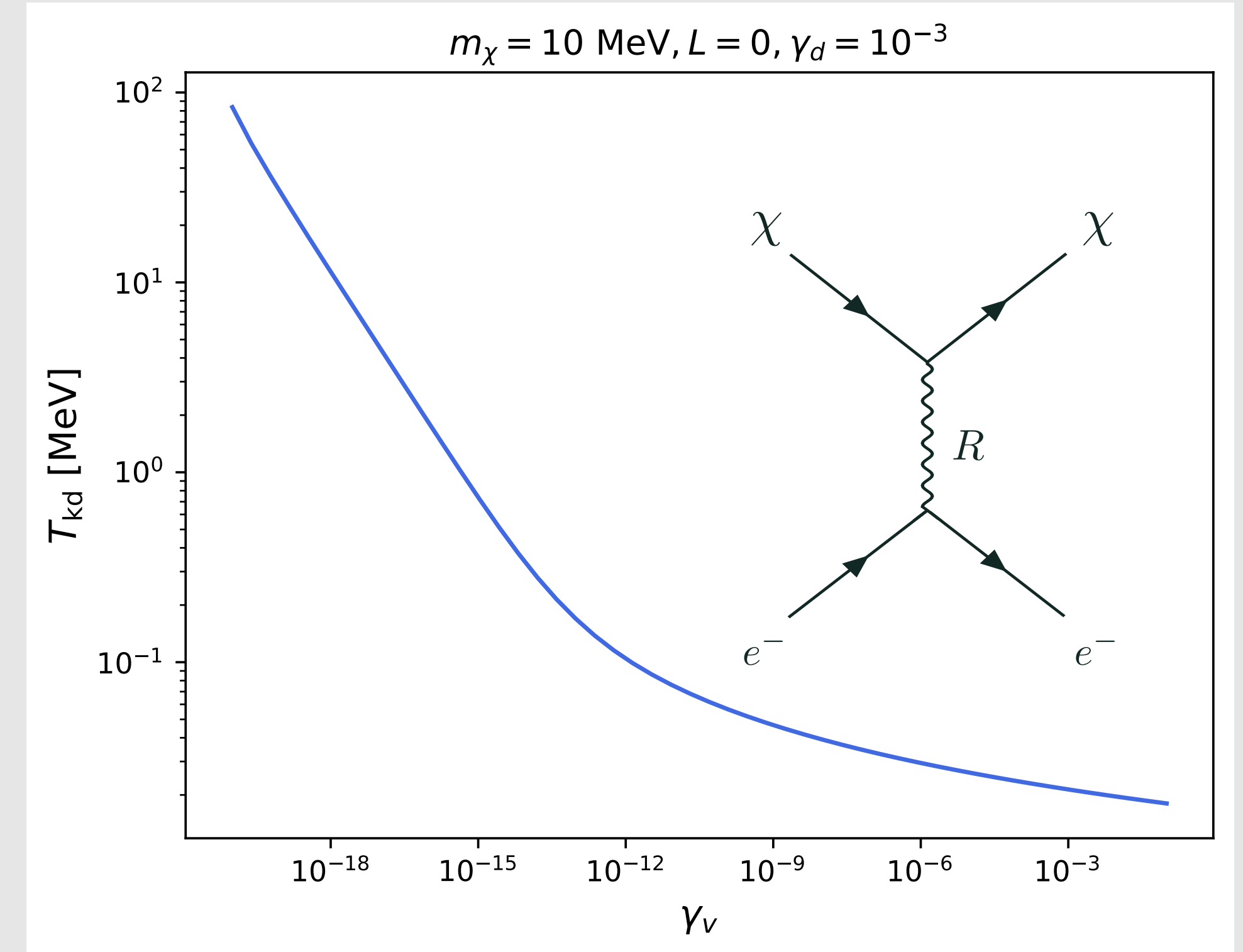
$$T_\chi(T) = \begin{cases} T & \text{if } T > T_{\text{kd}} \\ T_{\text{kd}} R(T_{\text{kd}})^2 / R(T)^2 & \text{if } T < T_{\text{kd}} \end{cases}$$

Kinetic decoupling when **scattering** becomes **inefficient**, i.e. when

$$\Gamma = n_e \langle \sigma v \rangle_{\chi e \rightarrow \chi e} \Big|_{T=T_{\text{kd}}} \lesssim H(T_{\text{kd}})$$

Scattering is related to annihilation via **crossing symmetry**

$$\sigma_{\chi e^- \rightarrow \chi e^-} = C \gamma_\nu \gamma_d \frac{p^2}{m_\chi^4}, \quad C = \mathcal{O}(1) \quad T \gtrsim m_e$$

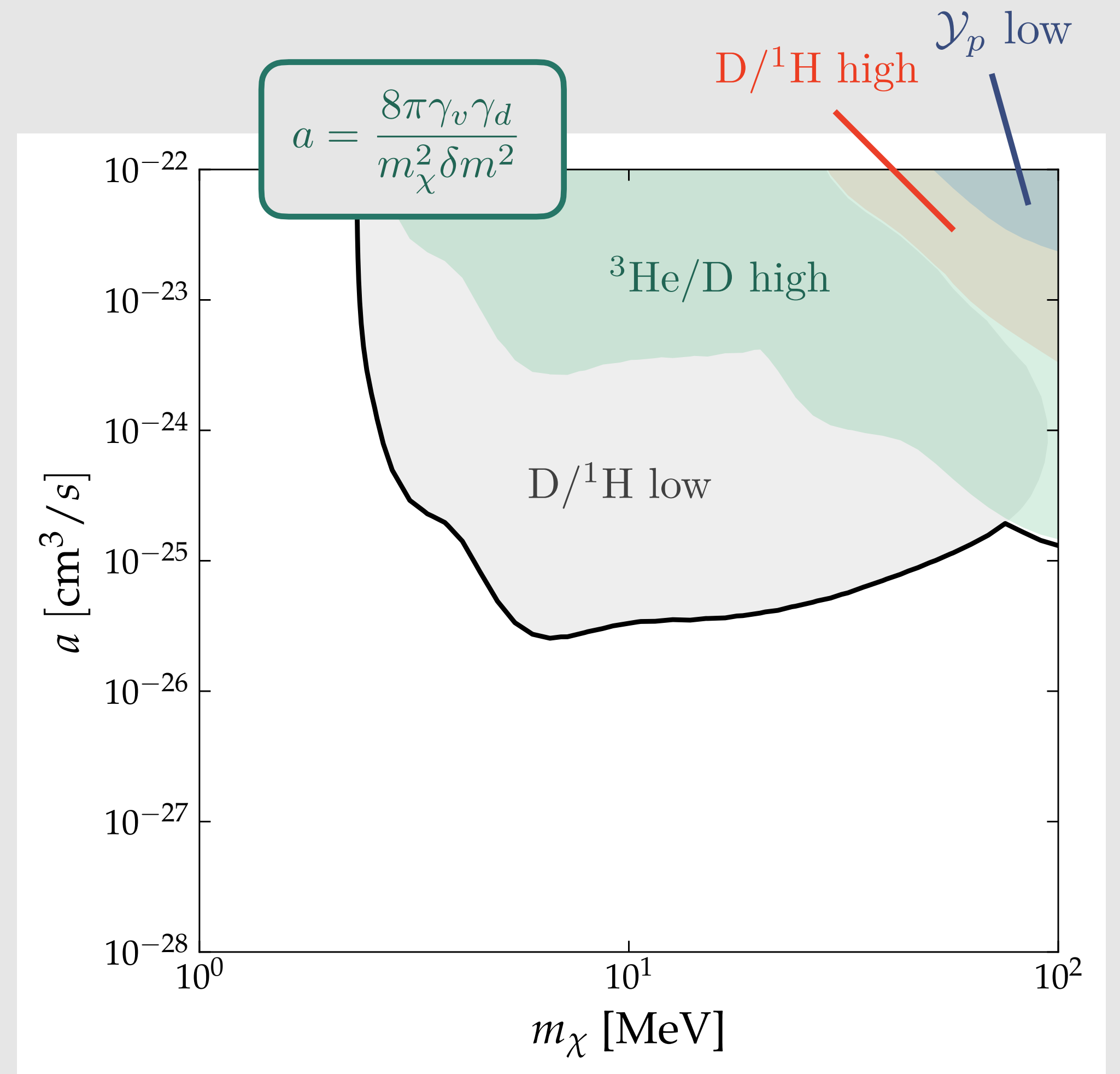


Results: single parameter space point

Use BBN observations

$$\mathcal{Y}_p = 0.245 \pm 0.003,$$
$$D/{}^1\text{H} = (25.47 \pm 0.25) \times 10^{-6} \quad \text{PDG (2022)}$$
$${}^3\text{He}/\text{D} = (8.3 \pm 1.5) \times 10^{-1} \quad \text{Geiss and Gloecker (2003)}$$

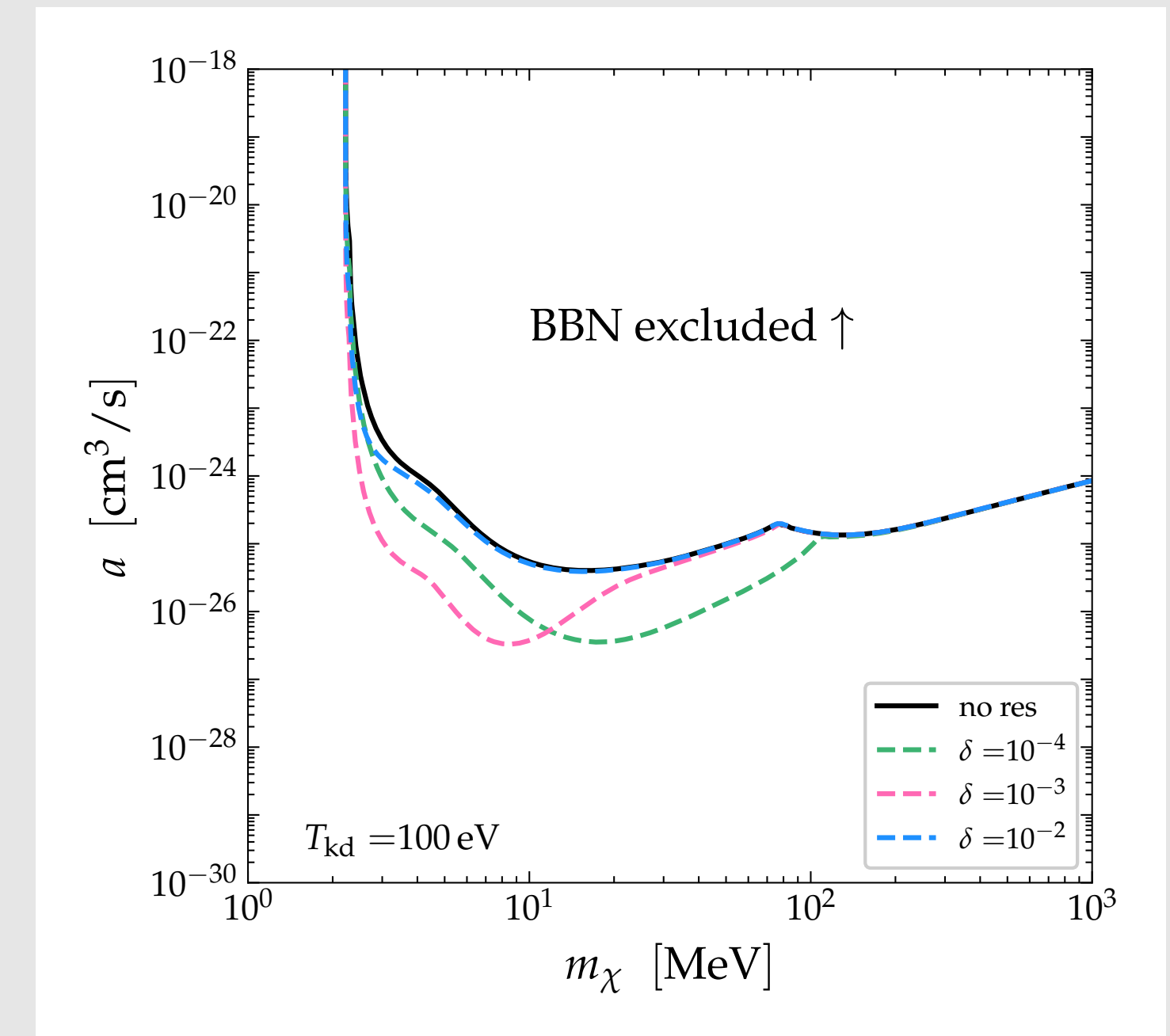
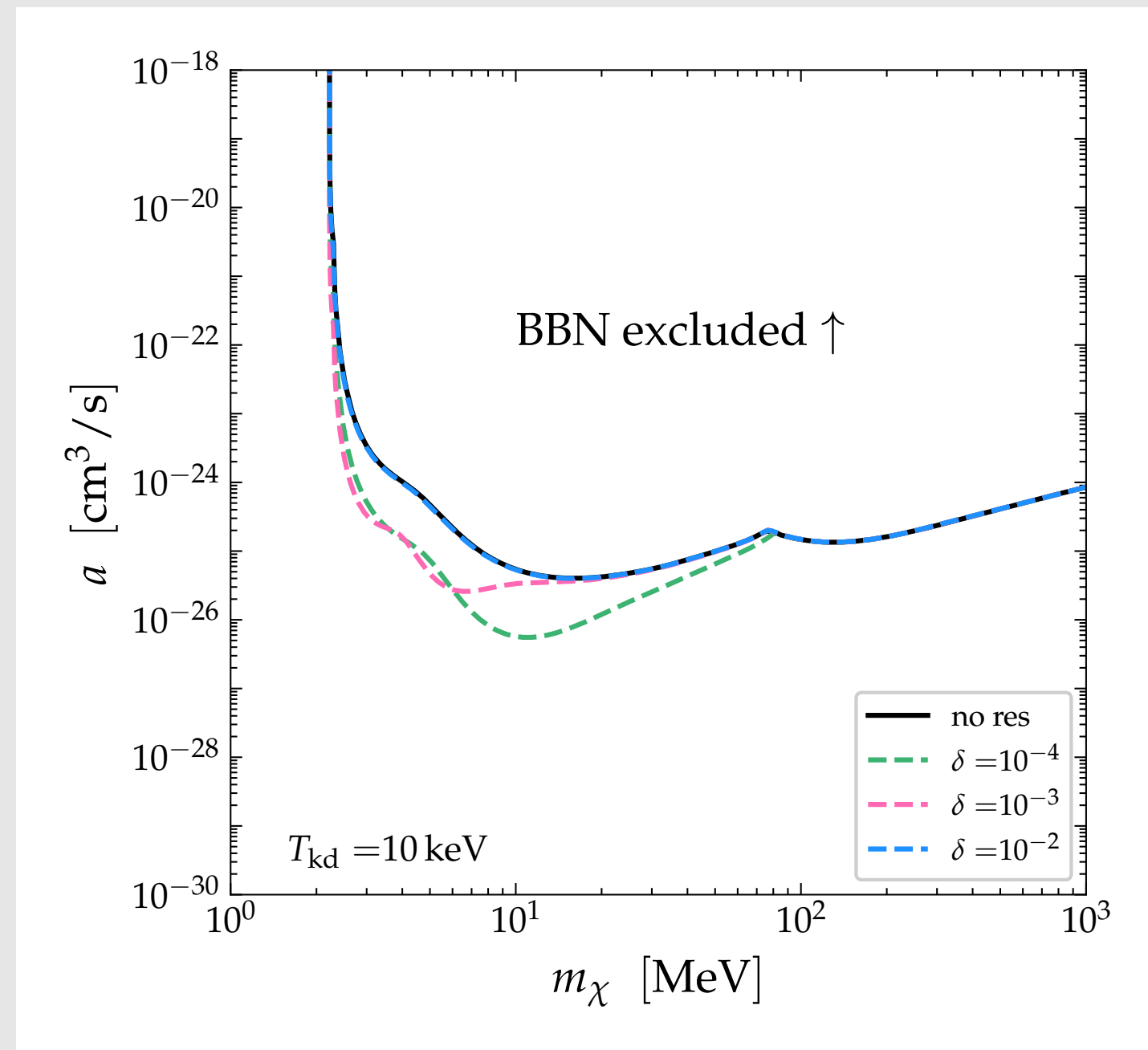
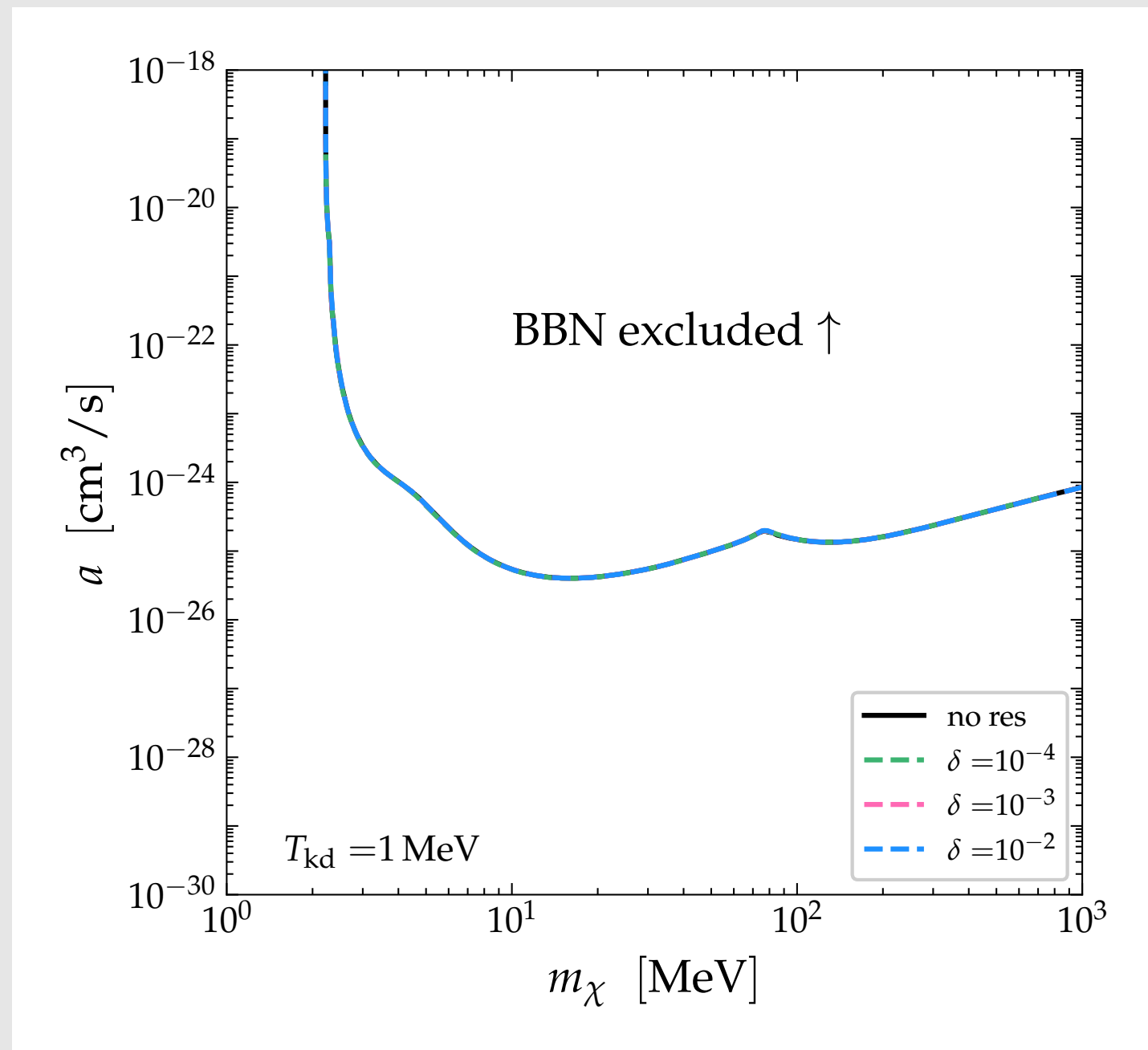
Deuterium abundance is most sensitive to the photodisintegration



Results (s -wave)

$$a = \frac{8\pi\gamma_v\gamma_d}{m_\chi^2\delta m^2}$$

Fixed T_{kd} : resonance effect is observable if the decoupling temperature is low enough



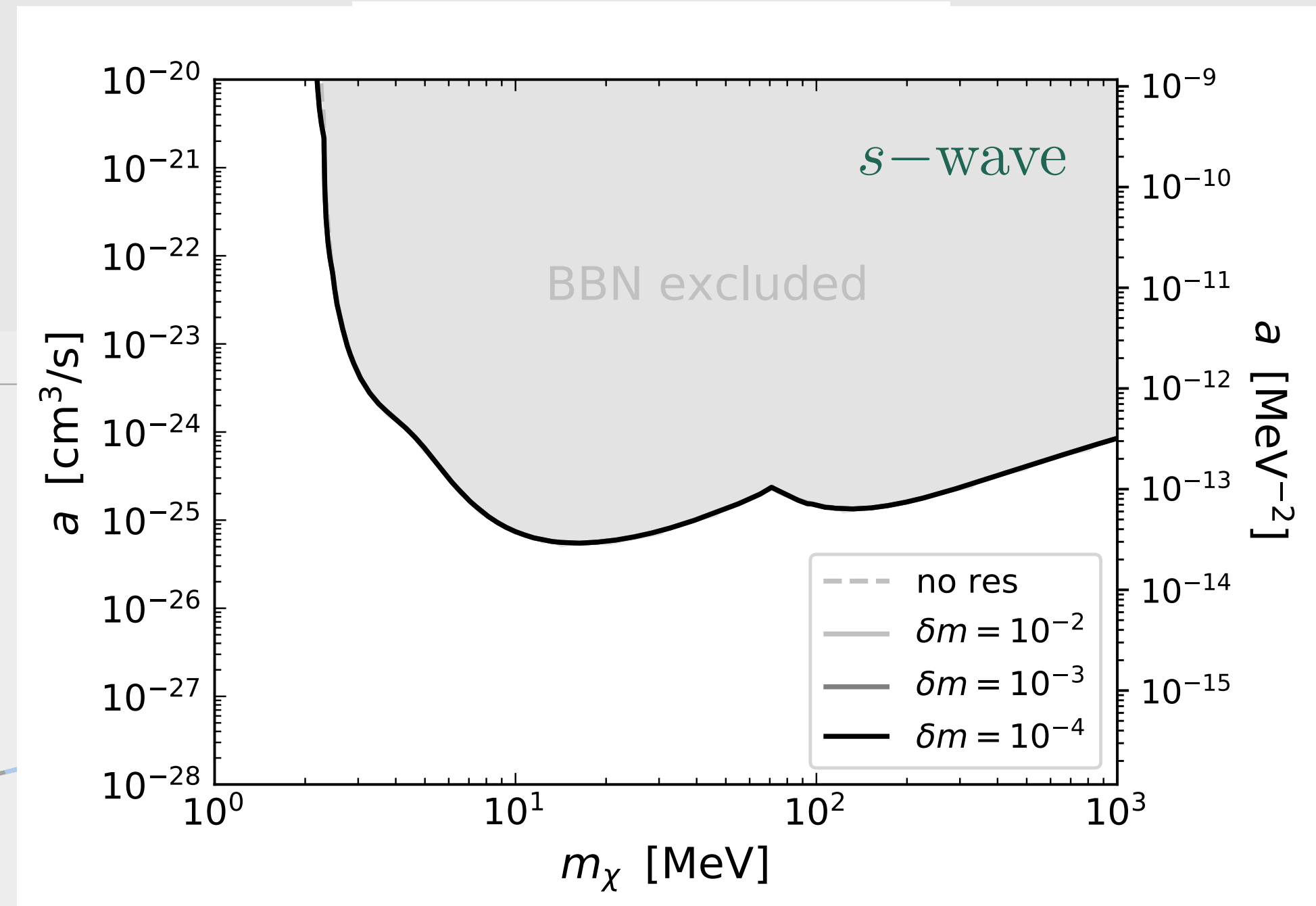
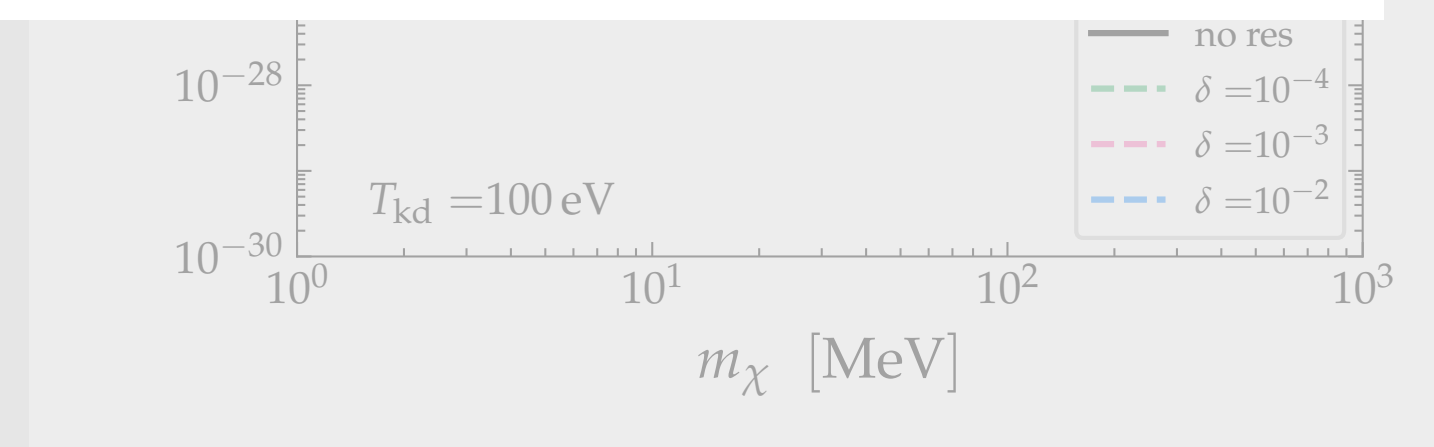
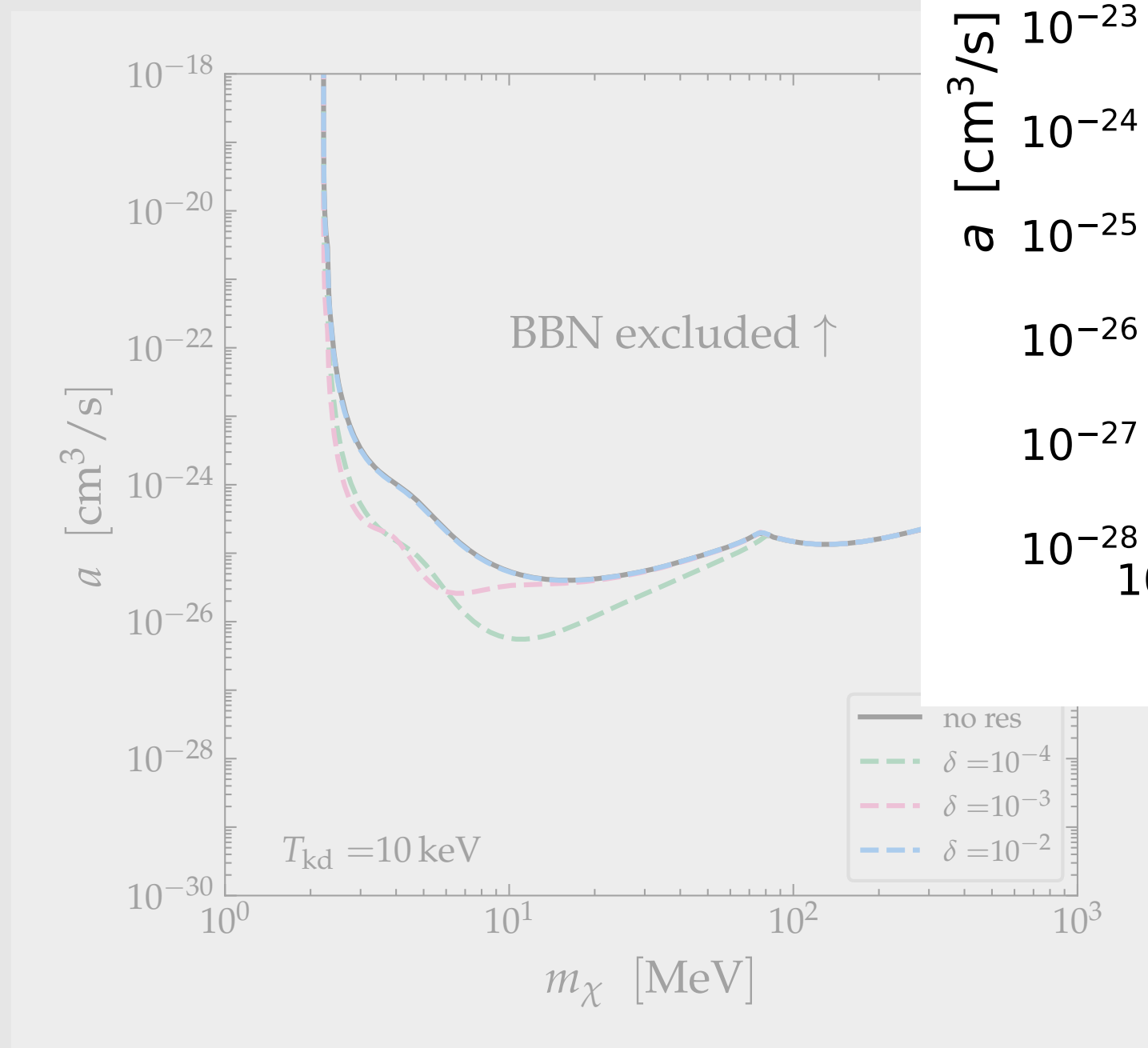
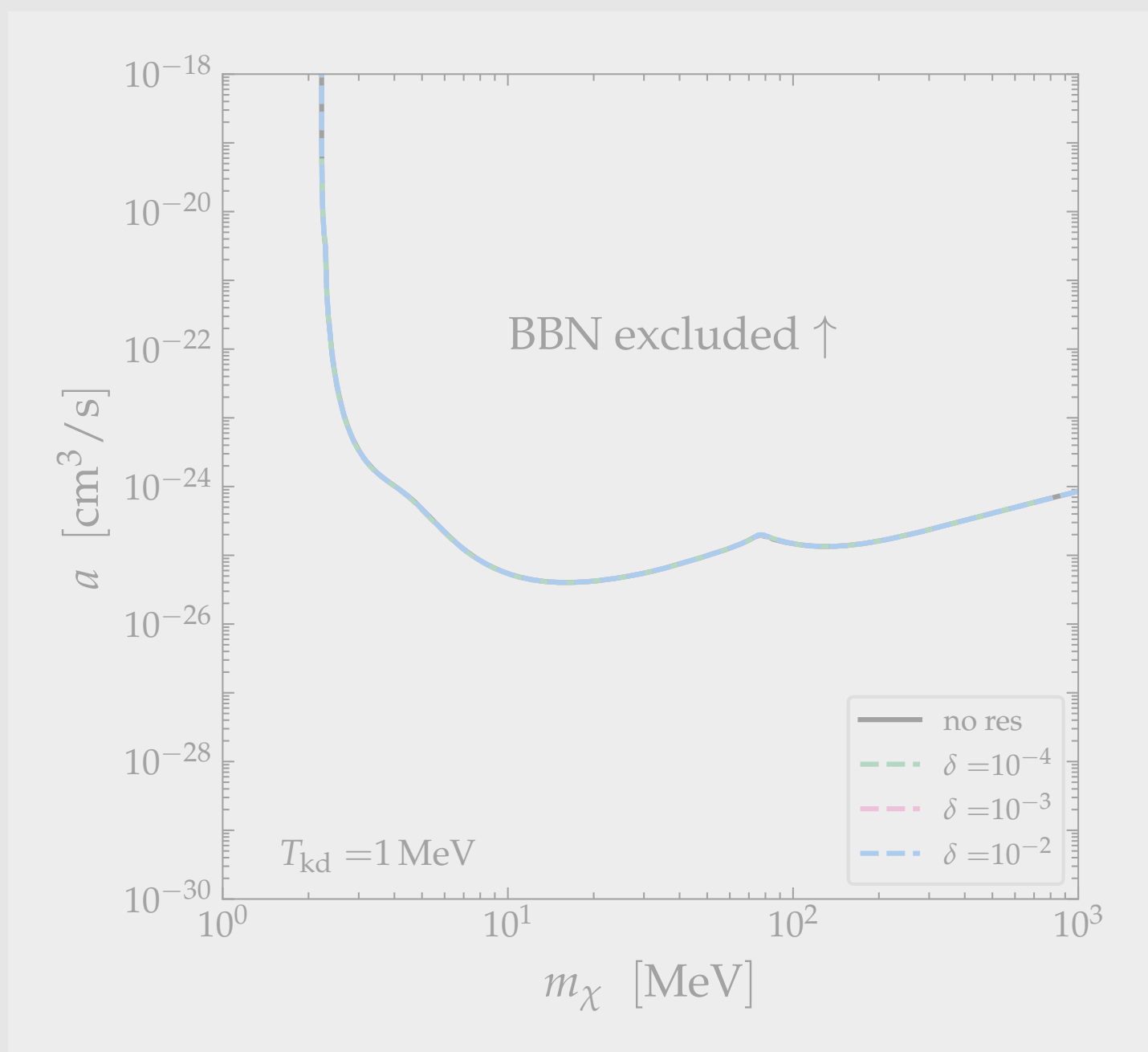
Results (*s*-wave)

$$a = \frac{8\pi\gamma_v\gamma_d}{m_\chi^2\delta m^2}$$

Fixed T_{kd} : resonance effect is observable if the decoupling temperature is low enough

Dynamically determined T_{kd} : the resonance is not effective as $T_{kd} \gtrsim 1 \text{ MeV}$

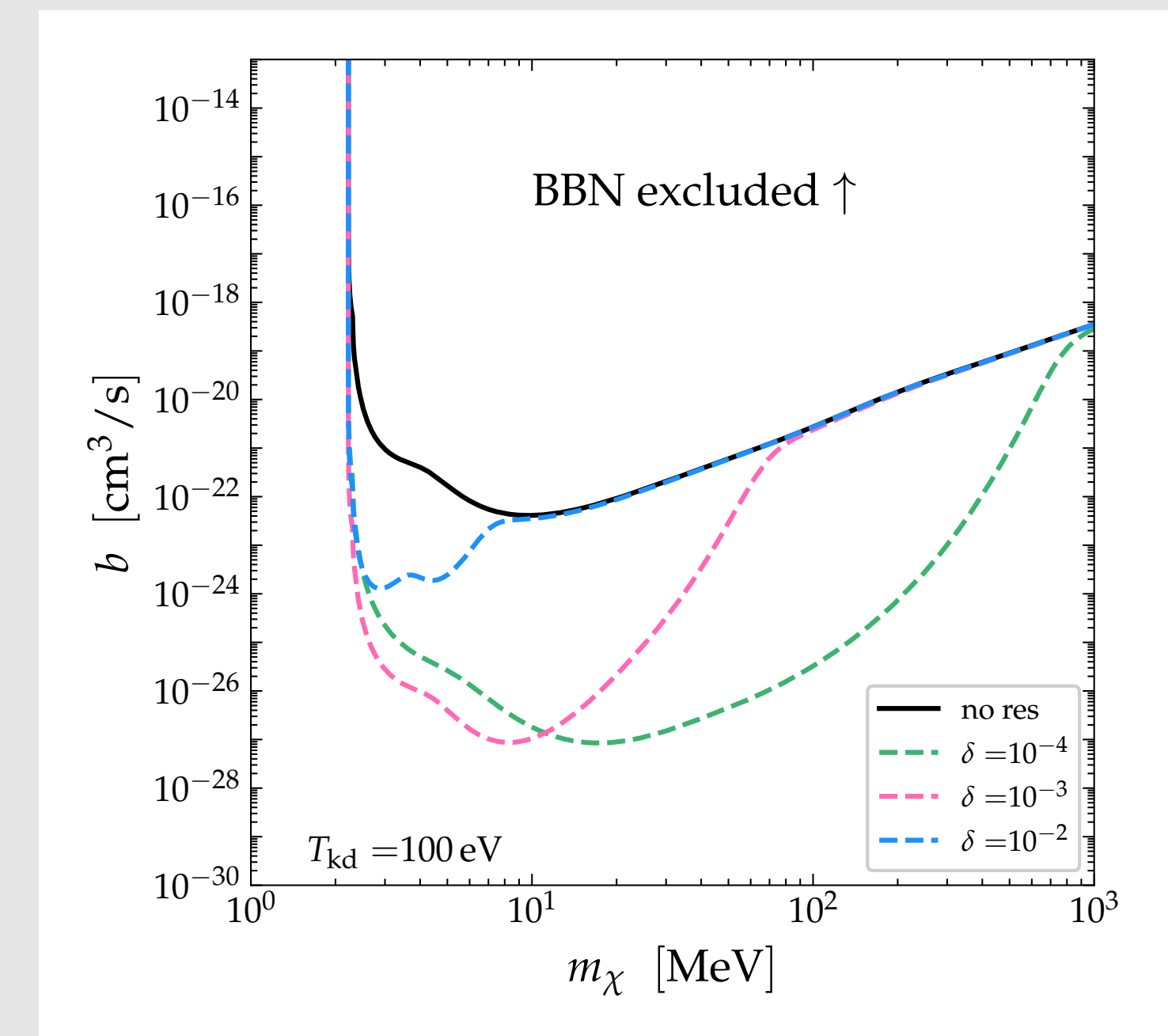
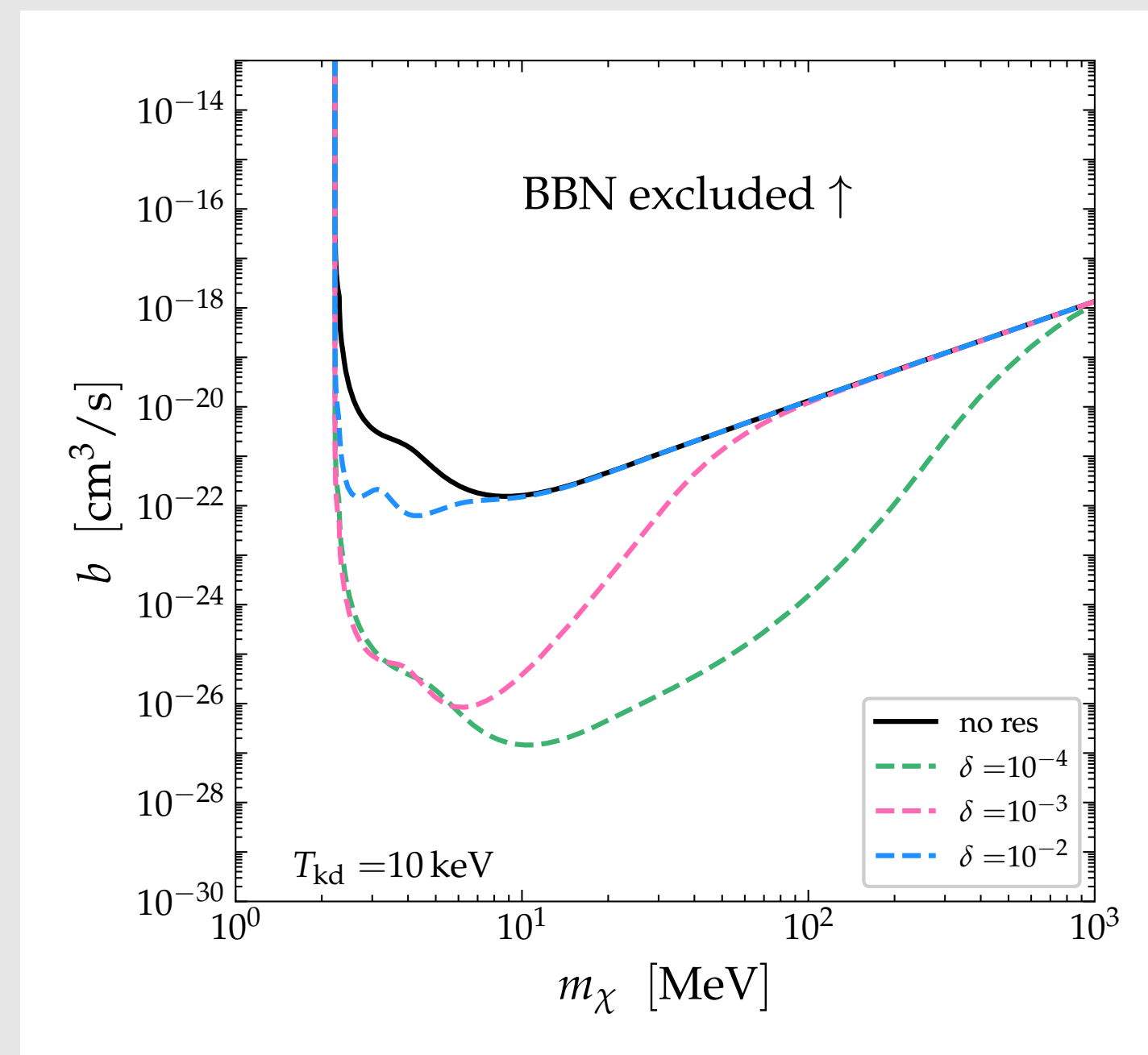
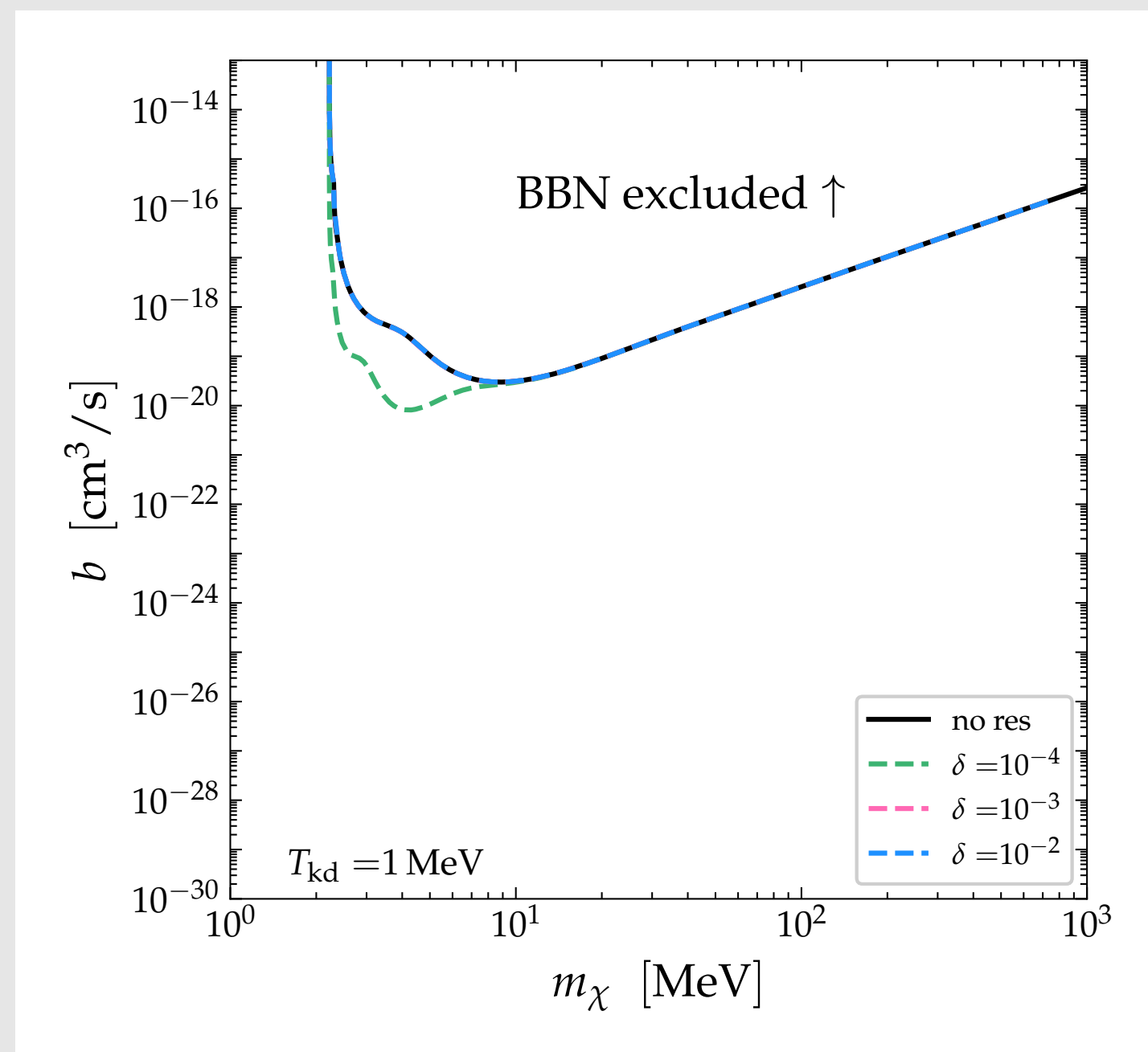
High decoupling temperature pushes the resonance outside the photodisintegration window



Results (*p*-wave)

$$b = \frac{2\pi\gamma_v\gamma_d}{m_\chi^2 \delta m^2}$$

For *p*-wave, the resonance effect is typically stronger



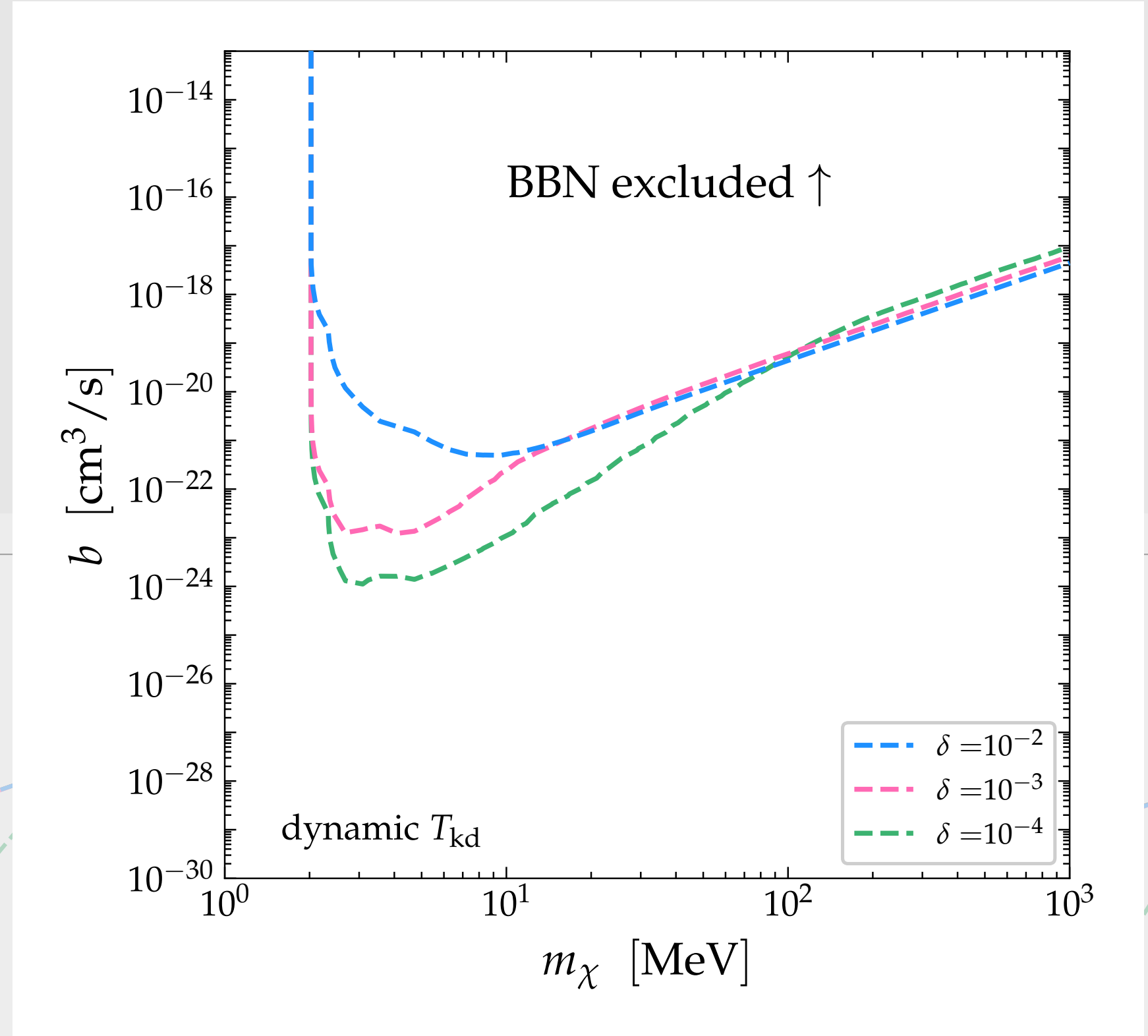
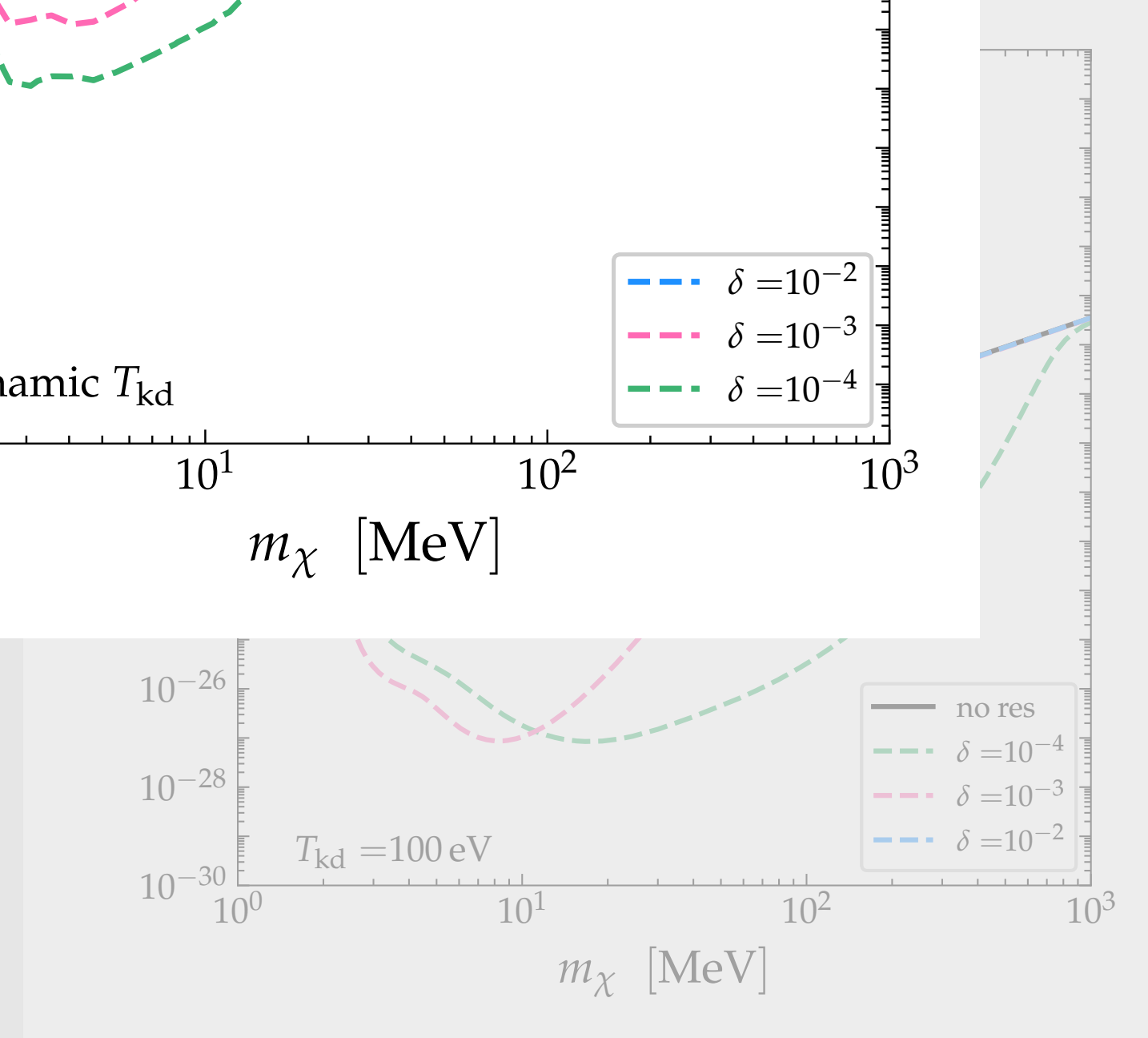
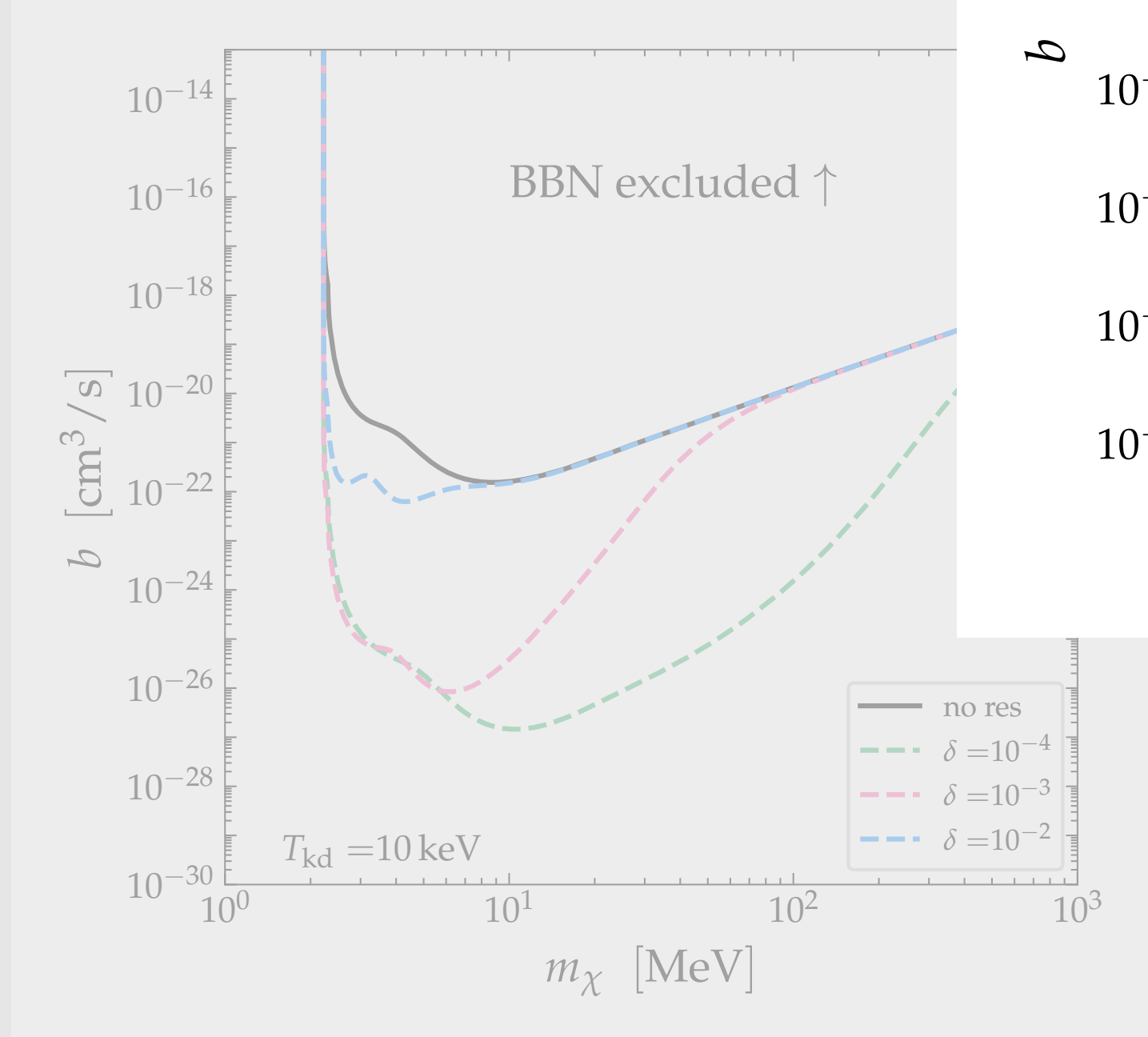
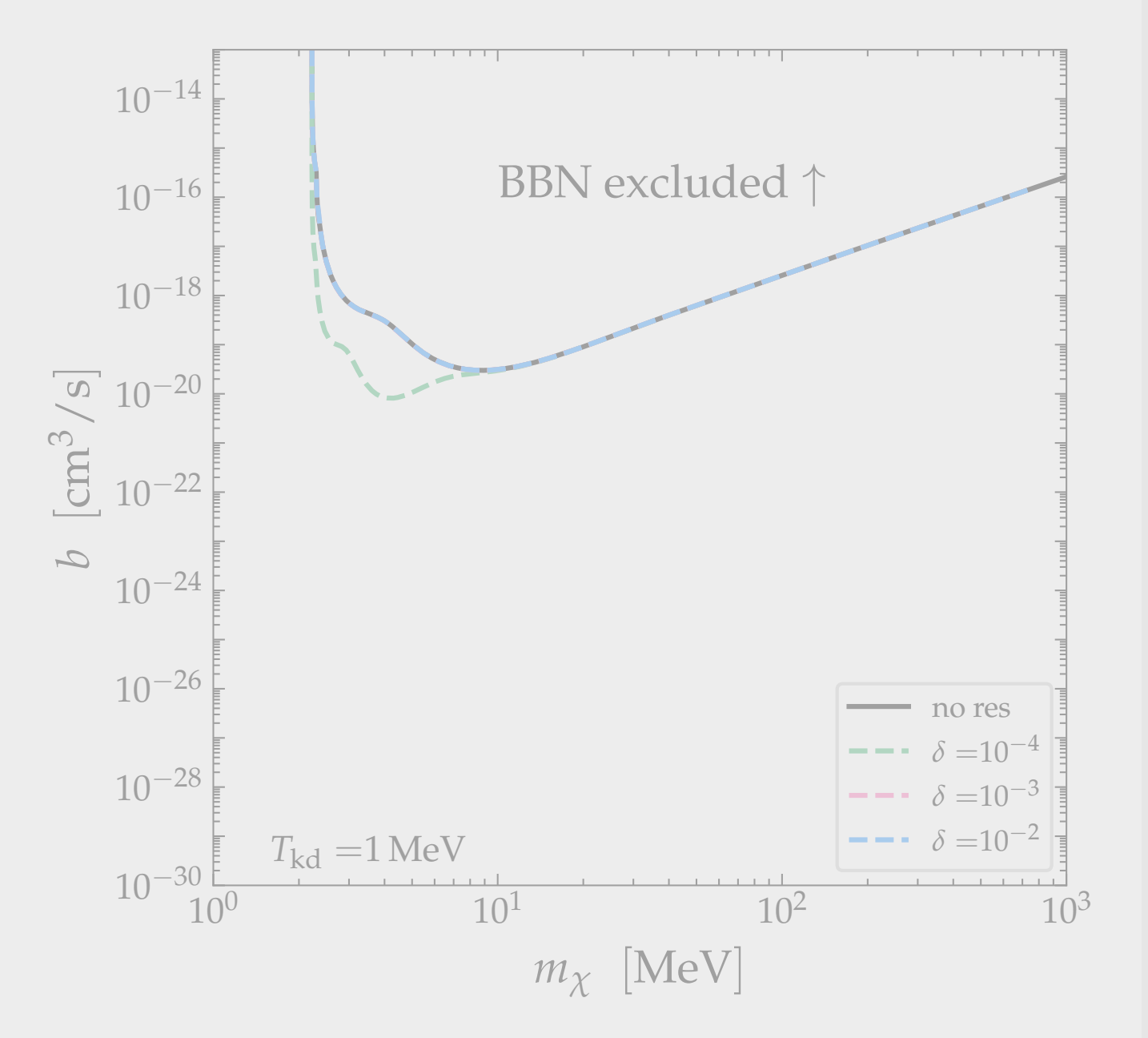
Results (*p*-wave)

$$b = \frac{2\pi\gamma_v\gamma_d}{m_\chi^2 \delta m^2}$$

Bounds are weaker than *s*-wave, so later decoupling

For *p*-wave, the resonance effect is typically stronger

Dynamical T_{kd} : resonance models are more strongly constrained compared to vanilla annihilations



Conclusions

- BBN observations can place **stringent bounds** on exotic energy injection in the early universe, such as (**resonant**) s - or p -wave DM annihilations
- **Decoupling temperature** greatly **impacts** the **constraints**; if in thermal equilibrium long enough, resonance model suffers from stronger bounds
- Determining the **decoupling dynamically**, s -wave resonance does **not** suffer from **increased bounds**, whereas p -wave does
- Want to use the code yourself? Will be included in an upcoming version of **ACROPOLIS**: check the [GitHub!](#)



Thank

you!

Back up

Intermezzo: core vs cusp

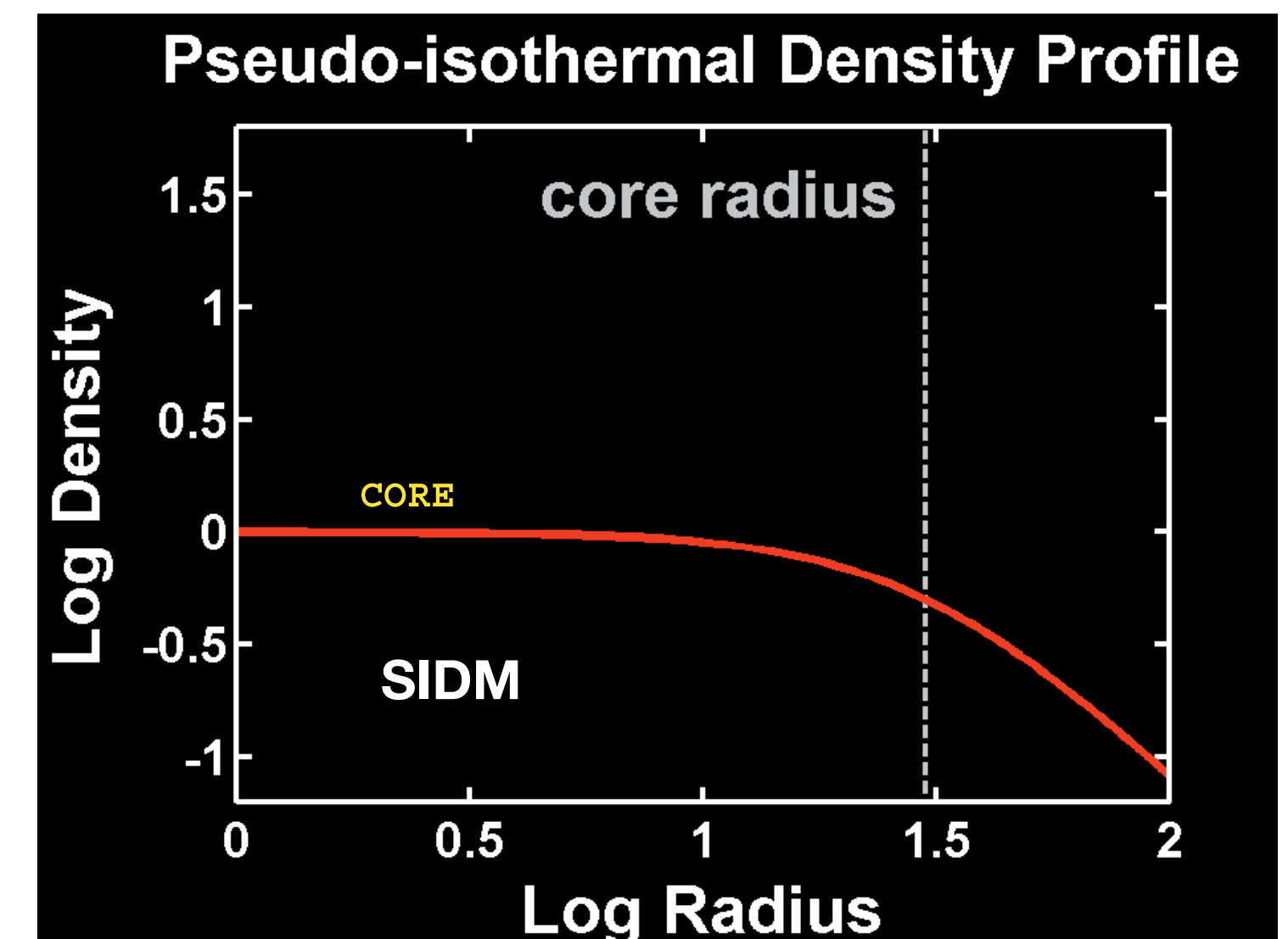
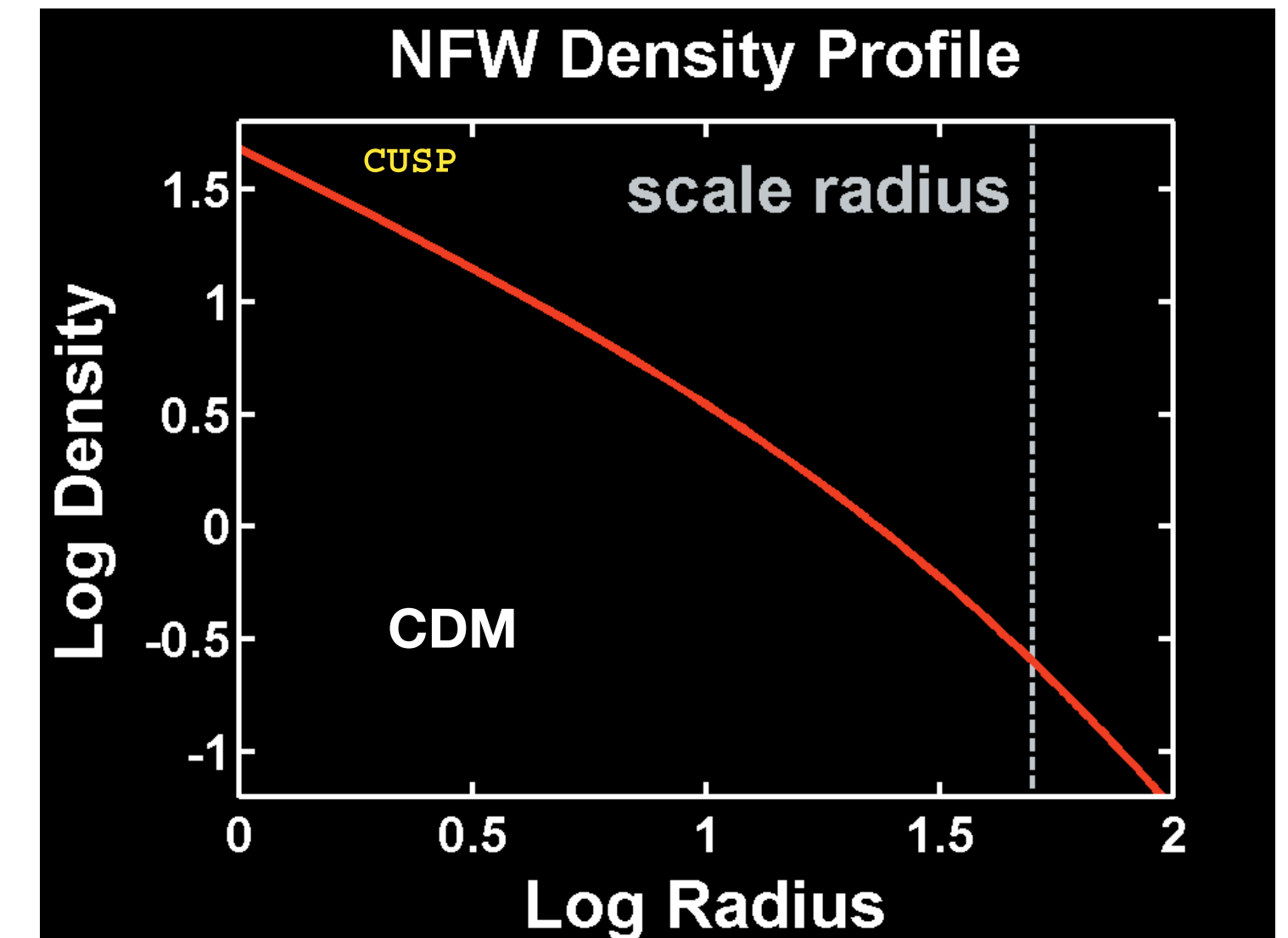
DM self-interactions change the shape of DM density profiles

Collisionless dark matter (CDM) predicts Navarro-Frenk-White profile

$$\rho(r)^{\text{NFW}} \propto (r/r_s)^{-1} (1 + r/r_s)^{-2}$$

Self-interacting DM (SIDM) predicts core-like profile: NFW away at large r , in center efficient heat transfer (isothermal)

$$\rho(r)^{\text{SIDM}} \propto \begin{cases} \text{const.} & r \ll r_1 \\ \rho(r)^{\text{NFW}} & r \gg r_1 \end{cases}$$



Del Popolo et al. [2209.14151]

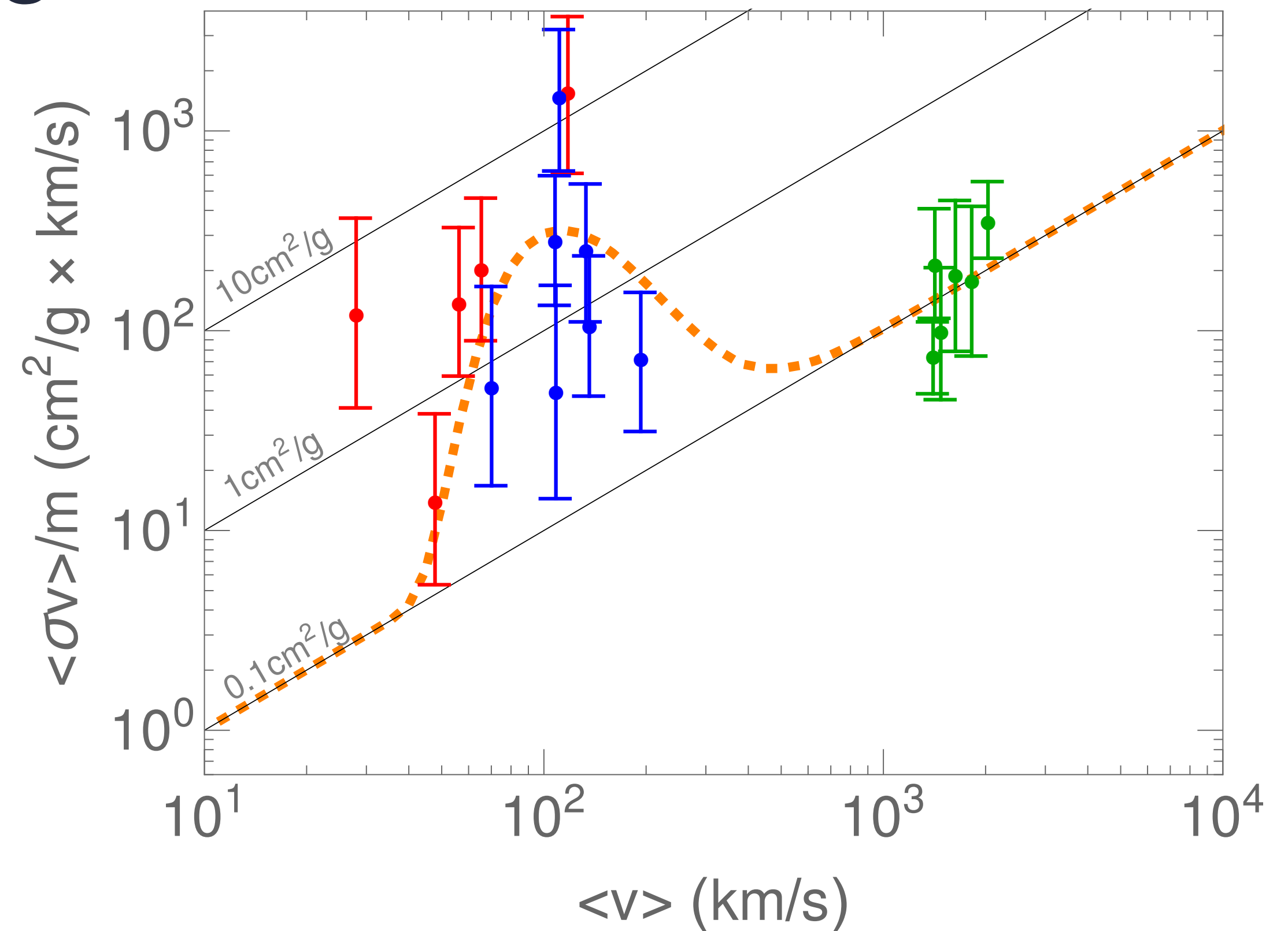
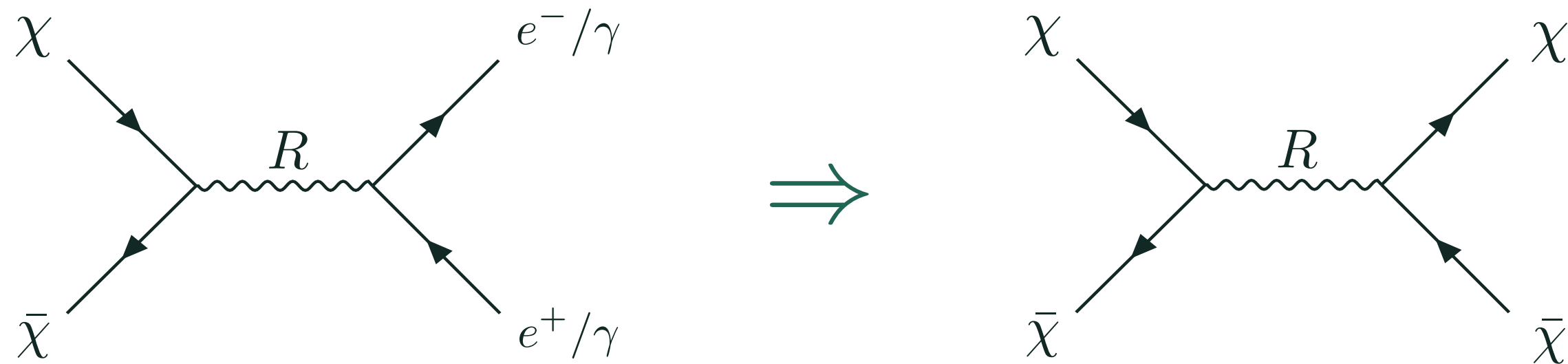
Intermezzo: resonant self-scattering

DM density profiles prefer SIDM models with strength

$$\frac{\sigma}{m} \sim 0.1 - 1 \text{ cm}^2/\text{g}$$

and velocity dependence to accommodate observations at different scales

For any electrophilic model, we also expect (sizeable) self-interactions



Adapted from Chu et al. [1810.04709]

Typical velocity peaks at galaxy halo sizes, which dictates mass of resonance

$$v_R \equiv 2\sqrt{\delta m} \sim 10^2 \text{ km/s} \Rightarrow \delta m \sim 10^{-8}$$

Photodisintegration window

Light element abundances $N \in \{n, p, D, {}^3\text{H}, {}^3\text{He}, {}^4\text{He}, {}^7\text{Li}, {}^7\text{Be}\}$

Photodisintegration is sensitive to specific **temperature range**

At early times **highly energetic photons** are **rapidly depleted** from pair creation

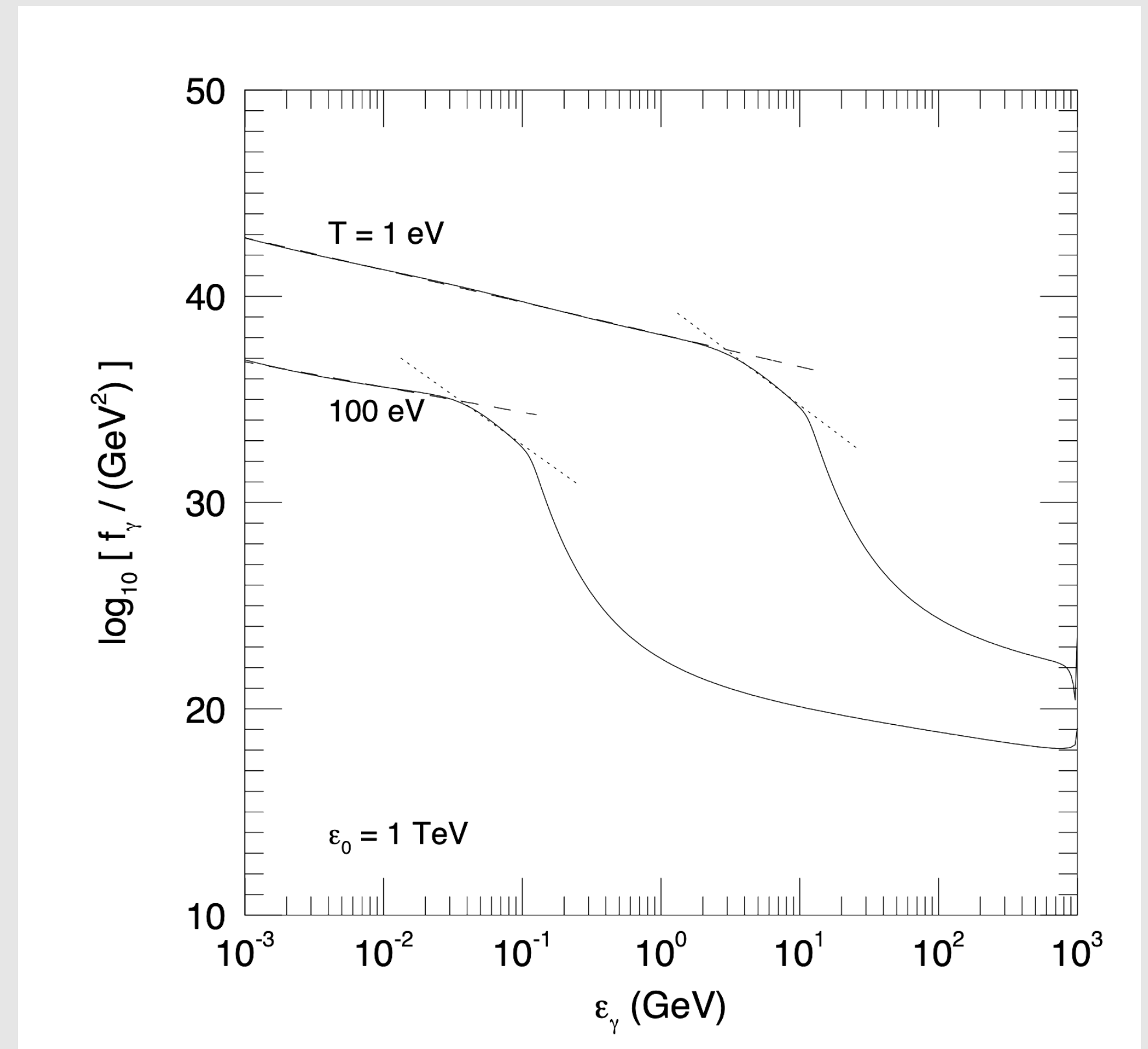


Temperature threshold is

$$E_{e^+e^-}^{\text{th}} \simeq \frac{m_e^2}{22T}$$

At late times, the DM fluid is too diluted for effective annihilations

$T \in [10^{-7}, 10^{-2}]$ MeV : well **after standard BBN** has ended



from Kawasaki and Moroi (1995) [astro-ph/9412055]

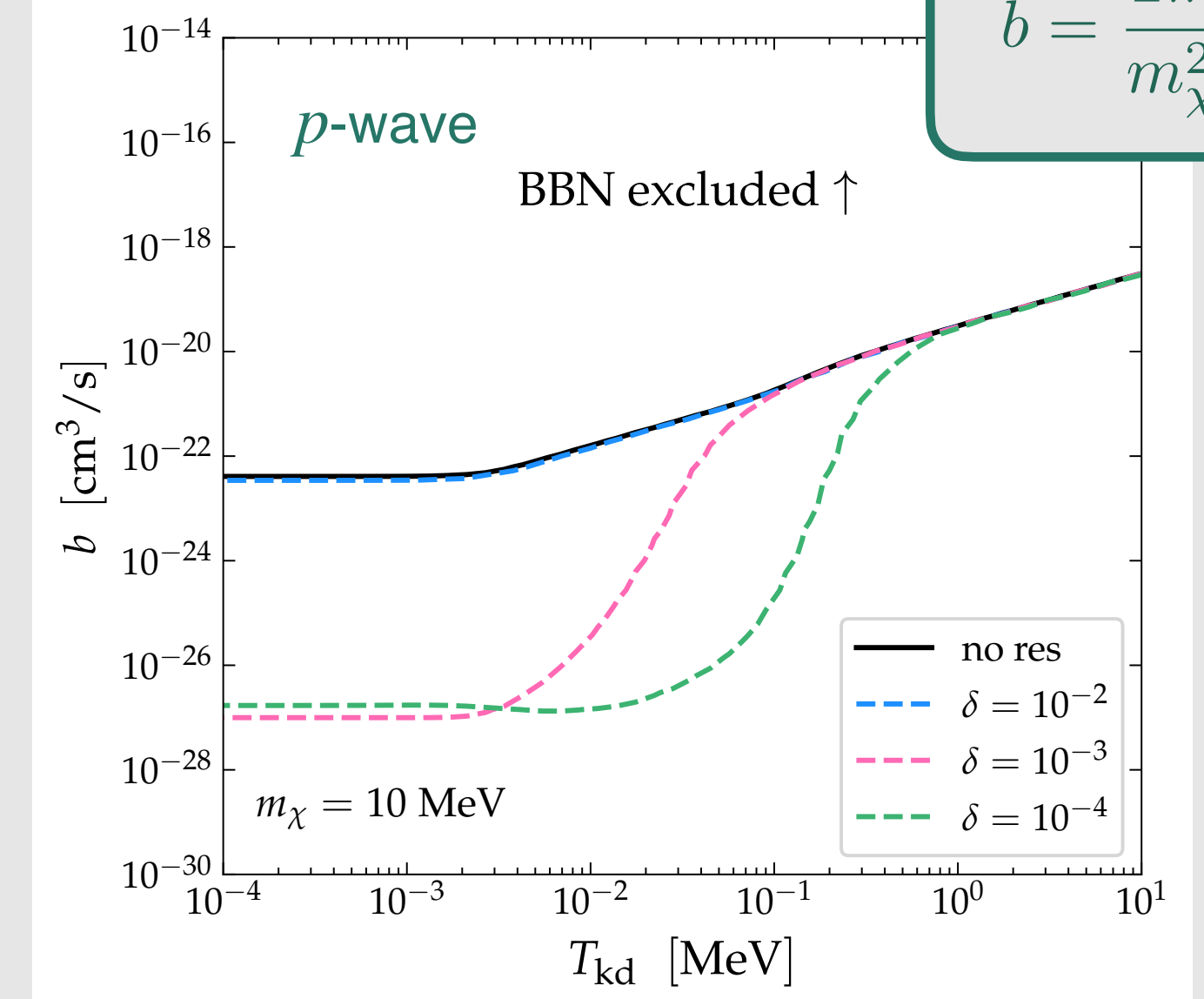
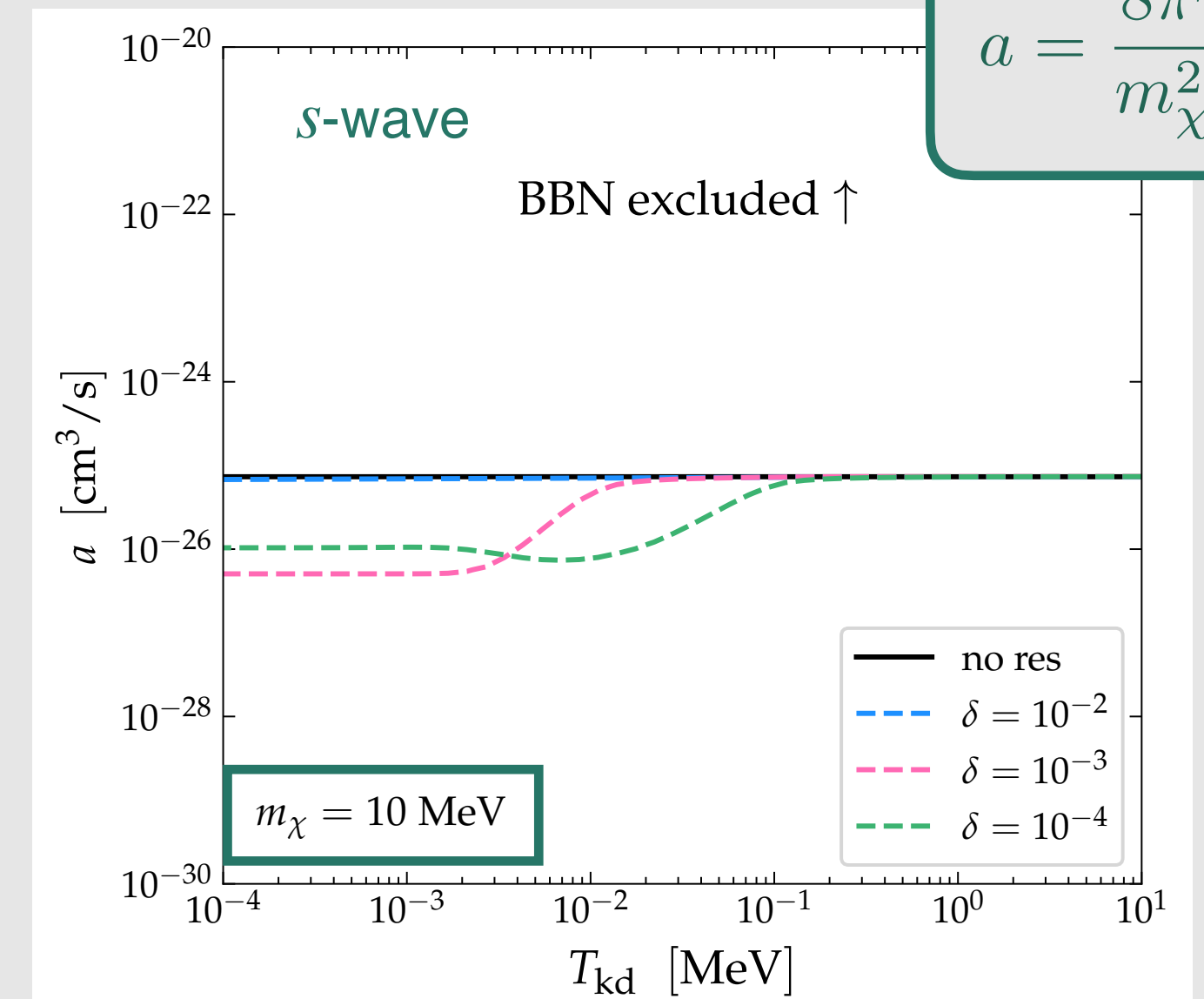
T_{kd} dependence

$$T_\chi(T) = \begin{cases} T & \text{if } T > T_{\text{kd}} \\ T_{\text{kd}} R(T_{\text{kd}})^2 / R(T)^2 & \text{if } T < T_{\text{kd}} \end{cases}$$

Setting the stage: understand the **decoupling temperature dependence** first

Low masses: **early decoupling suppresses resonance effect**

If **decoupling happens significantly late**, resonance model suffers from **stronger bounds**



T_{kd} dependence

$$T_\chi(T) = \begin{cases} T & \text{if } T > T_{\text{kd}} \\ T_{\text{kd}} R(T_{\text{kd}})^2 / R(T)^2 & \text{if } T < T_{\text{kd}} \end{cases}$$

Setting the stage: understand the **decoupling temperature dependence** first

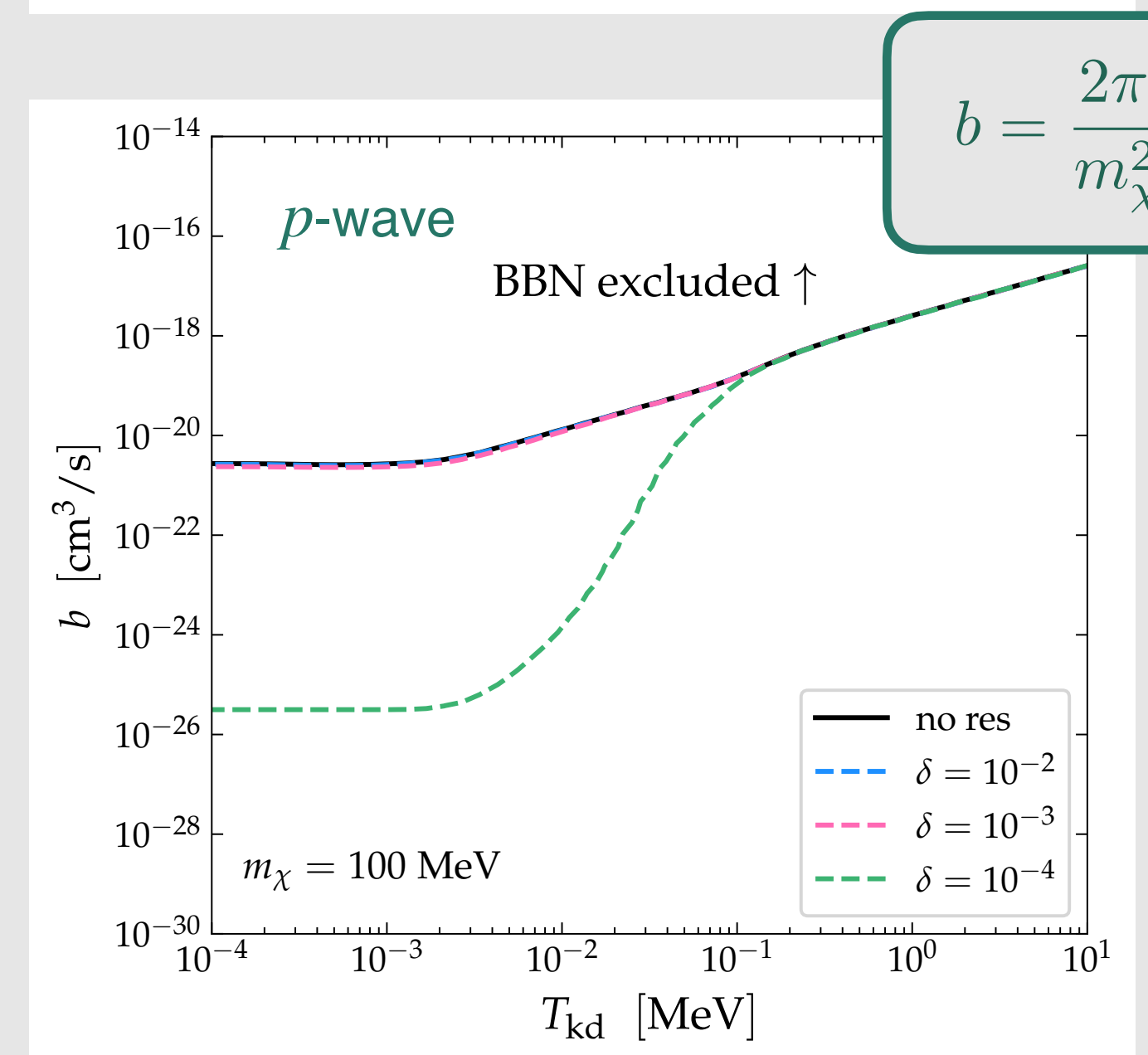
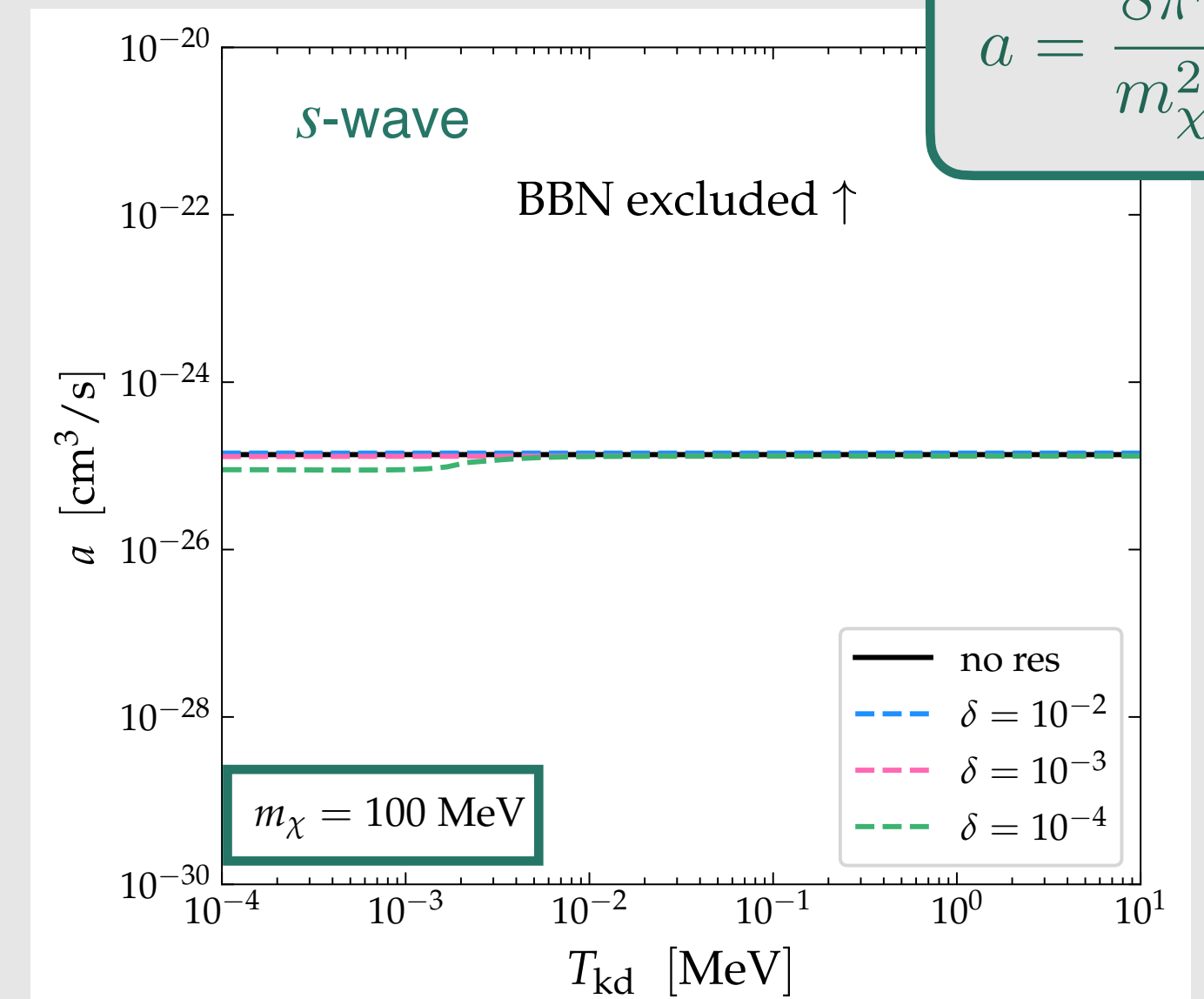
Low masses: **early decoupling suppresses resonance effect**

If **decoupling happens significantly late**, resonance model suffers from **stronger bounds**

Larger masses: **s -wave resonance barely noticeable**

For p -wave, the **narrow resonances are strongly constrained**

Across the board: **larger masses are typically less constrained**



Comparison to other bounds

p-wave results can be quite strict

Comparing the dark photon + scalar model

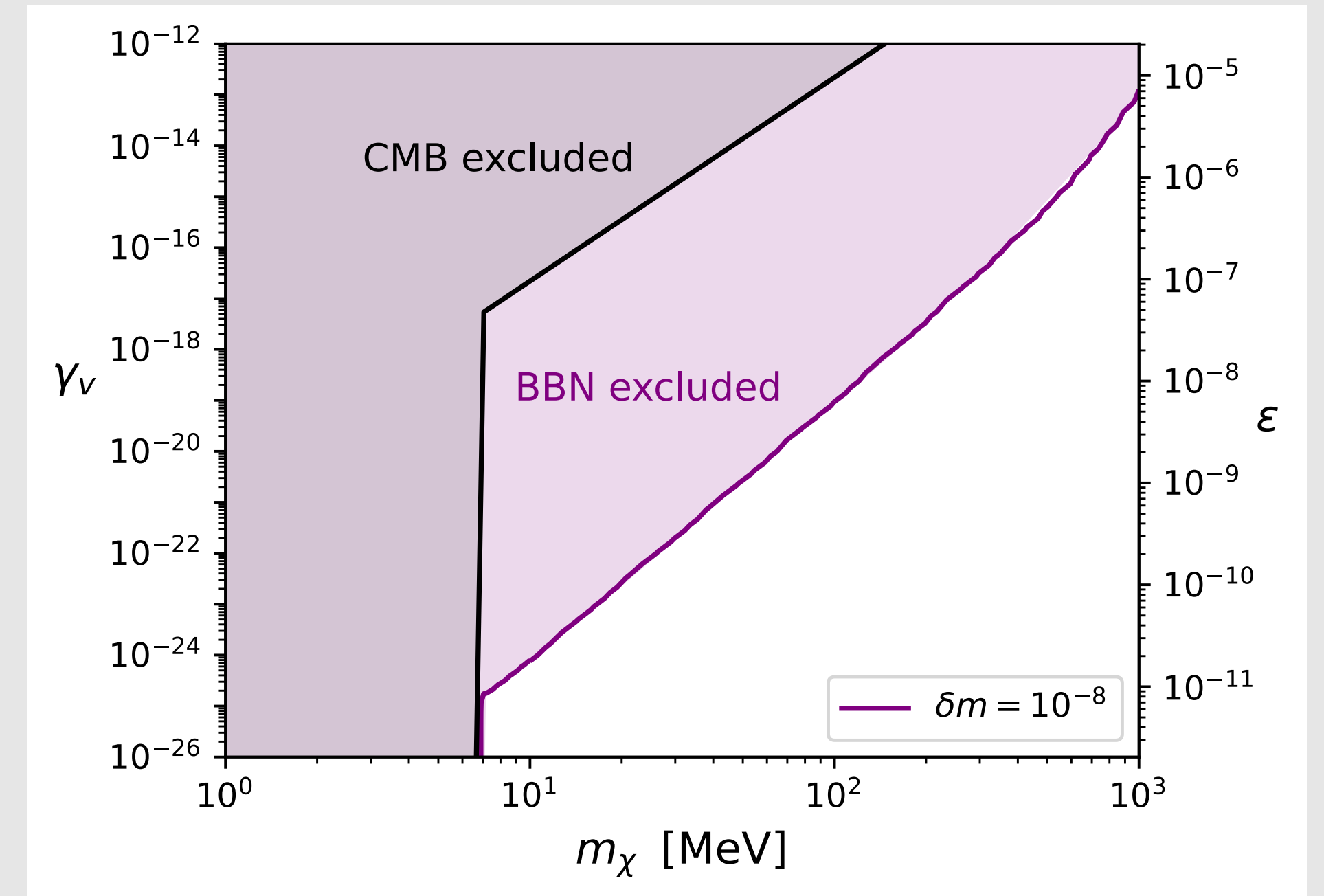
model	Lagrangian	n_d	γ_d	γ_v
2 scalar	$g_1 S S \Phi + g_2 \bar{e} e \Phi$	0	$\frac{g_1^2}{64\pi m^2}$	$\frac{g_2^2}{8\pi}$
scalar + vector	$g_1 \varphi^\dagger \overset{\leftrightarrow}{\partial}_\mu \varphi A'^\mu + g_2 \bar{e} \gamma^\mu e A'_\mu$	1	$\frac{g_1^2}{48\pi}$	$\frac{g_2^2}{12\pi}$
fermion + vector	$g_1 \bar{\chi} \gamma^\mu \chi A'_\mu + g_2 \bar{e} \gamma^\mu e A'_\mu$	0	$\frac{g_1^2}{8\pi}$	$\frac{g_2^2}{12\pi}$

and parametrizing the visible coupling $g_2 = \epsilon e$

Comparing this model to CMB constraints

$$p_{\text{ann}} = \frac{12\pi\gamma_v\gamma_d}{m_\chi^3 \delta m^2} \frac{T_{\text{SM}}^2}{m_\chi T_{\text{kd}}} < 3.3 \times 10^{-31} \text{ cm}^3 \text{ s}^{-1} \text{ MeV}^{-1}$$

Planck collaboration (2020)



BBN constraints are more strict than CMB, and can probe kinetic mixings down to 10^{-11} !

Why are the $\delta m = 10^{-3}$ more stringent?

Appears to be a “coincidence”. Resonance and off-resonance contributions compete

